DESIGN OF PROPELLER SHROUDS FOR STATIC THRUST CONDITIONS BY METHOD OF SINGULARITIES

A THESIS

Presented to the

Faculty of the Graduate Division

By

Joseph A. Gappa, Jr.

In Partial Fulfillment

of the Requirements for the Degree

Master of Science in Aeronautical Engineering

Georgia Institute of Technology

December 1960

DESIGN OF PROPELLER SHROUDS FOR STATIC THRUST CONDITIONS

BY METHOD OF SINGULARITIES

Approved:

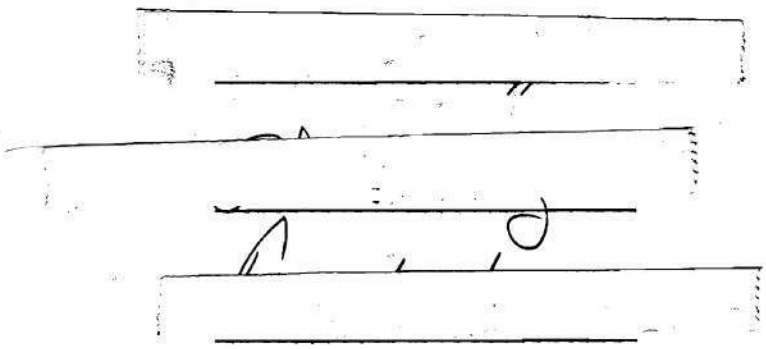

Date Approved by Chairman: Nov 11, 1960

"In presenting the dissertation as a partial fulfillment of the requirements for an advanced degree from the Georgia Institute of Technology, I agree that the Library of the Institution shall make it available for inspection and circulation in accordance with its regulations governing materials of this type. I agree that permission to copy from, or to publish from, this dissertation may be granted by the professor under whose direction it was written, or, in his absence, by the dean of the Graduate Division when such copying or publication is solely for scholarly purposes and does not involve potential financial gain. It is understood that any copying from, or publication of, this dissertation which involves potential financial gain will not be allowed without written permission.

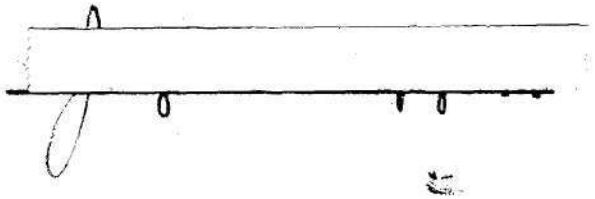

ACKNOWLEDGMENTS

The author expresses his appreciation to Professor Walter Castles, Jr., for suggesting the subject and for his invaluable guidance and assistance through all phases of this study. Gratitude is also extended to Doctor Robin B. Gray and Doctor Thomas W. Jackson for their review and comments on the material here presented.

TABLE OF CONTENTS

LIST OF TABLES

LIST OF FIGURES

LIST OF SYMBOLS

A	line integral of shroud bound vortex distribution along mean camber line of a shroud
c	chord length
P	arbitrary point
p	pressure at any point along shroud surface
p_o	ambient pressure
p_w	stagnation pressure in the wake
Q	mass flow, $Q = \rho \pi R_o^2 v$
R_o	ultimate wake and sink disk radius
r	radial location from axis of symmetry
r_t	leading edge radius
T	propeller thrust
t	maximum thickness expressed as a fraction of the chord
V	free stream velocity
v	normal component of induced velocity at sink disk plane
V_t	rotational component of velocity due to torque of propeller
V_r	radial component of velocity at P(x, r)
v_r	radial component of velocity at P(x, r) (unit radius and strength)
V_x	axial component of velocity at P(x, r)
v_x	axial component of velocity at P(x, r) (unit radius and strength)
x	axial location, normal distance of P from sink disk plane
y_t	thickness distribution measured perpendicular to mean camber line
x/R_o	non-dimensional axial location
r/R_o	non-dimensional radial location

γ	wake-vortex-sheet strength, 2v, large distance downstream
Γ_n	strength of nth vortex ring spaced along mean camber line
θ	shroud contour expansion angle
ρ	mass density
ψ	stream function
ψ'	stream function for rotor flow pattern as computed using a uniform vortex cylinder for wake vortex system (replaced by a uniform distribution of sinks on a circular disk)
ψ_t	value of the stream function along the wake boundary
ψ_s	stream function for a uniform distribution of sinks over a circular disk
$\Delta\psi_n$	increment in ψ due to nth source ring along mean camber line

SUMMARY

The purpose of this investigation was to determine a systematic approach to a theoretical design of a shroud for a shrouded-propeller combination operating in the static thrust condition. The assumptions made were: steady flow, axial symmetry, and incompressible flow, so that the method of singularities could be used.

Results of this study show that a procedure can be established by which a shroud is designed for a given set of initial conditions. The procedure consists, first, of determining, from the initial conditions, an initially assumed mean camber line along which vortex rings of proper strength are superimposed and, secondly, of fitting the resulting boundary surface to a corresponding inner contour of a NACA Four Digit airfoil section, or some other known shape selected for the shroud inner surface. An extension of the boundary stream surface determines the outer contour.

An analysis of the two major subdivisions of the procedure referred to above, with a sample solution utilizing procedures developed, comprise the main section of this work.

For any given distribution of the singularities that are used, the velocity components at the surface of the shroud can be approximately determined.

CHAPTER I

INTRODUCTION

Theoretical methods for calculating shroud shapes are known in the case of a shrouded propeller with a free stream velocity. Basically, the principle involved is the selection of streamline of flow for any given free stream condition which passes through a desirable reference point for the shroud trailing edge, as, for example, a point located a distance equal to an assumed cylindrical wake radius from the axis of symmetry. Having selected a reference point, and since the Kutta conditions must be met, the trailing edge and the forward extension of the trailing edge stream surface furnishes the shroud mean camber line. An iterative process of bound vortex strength distribution along the initial and subsequent mean camber lines can be used to obtain the desired shape. The thickness distribution and the contour of the shroud can then be designed by methods given in references 1 and 2.

The problems of design are considerably complicated under the conditions of static thrust in that there is no leading edge stagnation point such as exists in the case where there is a free stream velocity. As a beginning in the design, some point along an assumed wake boundary can be arbitrarily selected as the trailing edge and serve as a reference point. Hence, with an arbitrarily fixed trailing edge, the problem of determining a proper length and shape of the mean camber line is the initial obstacle to the design of a propeller shroud under conditions of static thrust. Secondly, from a practical standpoint, the inner contour

of the theoretical shroud must subsequently be adjusted to some satisfactory curve.

The author is unaware of any theoretical methods available in the literature at this time for the design of propeller shrouds under conditions of static thrust. It is intended, therefore, to present a suitable means of design, under the assumptions of steady flow,[1] axial symmetry, and incompressible flow.

To find examples of practical needs for theoretical design of propeller shrouds under conditions of static thrust, one may turn to the general field of hovering-type aircraft and underwater devices with negligible forward velocities, which are of immediate concern and interest to the Armed Forces.

---

[1]Steady flow implies an idealized propeller with an infinite number of blades.

CHAPTER II

ANALYSIS

General Considerations.--Given the propeller thrust, the diameter of the wake, and with the assumption that the wake is cylindrical, the wake vortex sheet strength, γ , can be computed from the relationship

$$T = Q\gamma = \rho\pi R_o^2 v\gamma \qquad \text{where } v = \gamma/2$$

Then

$$T = \frac{\rho\pi R_o^2 \gamma^2}{2}$$

With the sheet strength known, the boundary surface can be plotted for the flow field, provided a shroud bound vortex strength distribution is placed along an assumed mean camber line. A procedure to be followed in determining the most suitable mean camber line with regard to length and shape will be covered in some detail later in this analysis. The process, though iterative, is systematic. Conditions satisfied by this iterative procedure are primarily two:

a. Determining a preliminary, first estimate, inner contour shape within limits of permissible shroud contour expansion angle measured from the vertical position and a tangent line to the shroud inner surface and passing through the selected reference point at the shroud trailing edge (see Figure 1).

b. Assuring negligible wake contraction up to some selected distance, say $3R_o/2$ below the horizontal plane passed through the reference point selected (see Figure 1).

The second major subdivision of the design problem is one of utilizing a procedure developed by Professor Walter Castles, Jr. and Dr. Robin Gray (reference 2). Following the steps of the method outlined, the inner contour of the unit stream surface (total value of the stream surface non-dimensionalized to unity) plotted for the above can be made to coincide with the desired inner contour of a known airfoil section. The outer contour is outlined by extending the plot of the inner shroud surface streamline around to a desired cut off point (see Figure 2).

With a known shroud vortex distribution, the velocity components of the flow can be determined (reference 1). It follows, then, that for the assumed propeller having a very large number of blades, the pressure distributions along the surface of the designed propeller shroud can be found by application of Bernoulli's Theorem, which gives for the pressure, p, at any point (x, r) ahead of the propeller[1]

$$p_o - p = \frac{1}{2} \rho (V_x^2 + V_r^2)$$

For points behind the propeller it is necessary to substitute

$$p_w = \frac{1}{2} \rho \gamma^2 + p_o$$

for p_o in the above equation. The radial and axial velocity components, v_r, v_x for the vortex ring and uniform source distribution over a disk are given in tabular form by Kucheman and Weber (reference 1). Areas not covered in the tabular solutions can be solved for by methods outlined in the appendix of this reference.

---

[1]Pressure distribution formulas are approximate since the number of propeller blades is finite and the rotational component of velocity, V_t, due to torque, has been omitted.

Method of Singularities in Determining Stream Surfaces for Static Thrust.--The concept of the stream function in the two dimensional flow can be extended to axially symmetric flow without a free stream velocity. Further, it is shown in reference 1 that the flow field of a uniform sink distribution on a circular disk is identical to flow induced by a uniform vortex cylinder of constant strength and semi-infinite length except for a region inside the wake where a velocity component equal to the strength of the bounding vortex sheet must be added. Considering then, the value of the stream function, ψ', for the flow due to the vortex cylinder

$$\psi' = \pi r^2 \gamma - \psi_s$$

for the region inside the wake and below the plane of the sink disk and $\psi' = \psi_s$ for the region outside the wake (see Figure 3), on the boundary of the ultimate wake the value of the stream function is $\psi' = \pi R_o^2 \gamma$. However, since the axial component of the induced velocity at the sink disk plane is $v = \gamma/2$, it follows that at the sink disk boundary $\psi' = \pi R_o^2 \gamma/2$ or a "deficit" exists in the volume flow. Deficit $= \pi R_o^2 (\gamma - v) = \pi R_o^2 \gamma/2$. The deficit at any point along the assumed cylindrical wake boundary can be determined by subtracting from ψ of the ultimate outer wake boundary the computed value of ψ'. This quantity must be adjusted to zero by the propeller shroud and is a function of the wake vortex sheet strength. For example, the deficit at the trailing edge of the proposed shroud is

$$\psi - \psi' = \pi R_o^2 (\gamma - \gamma/2) = \pi R_o^2 \gamma/2$$

The values of the stream function for a vortex ring, having a unit strength and a unit radius, have been calculated by Kucheman and Weber, and are given as Table 3, reference 1. Also given in reference 1 are the velocity components, v_r, v_x for the unit strength vortex ring having a unit radius (reference 1, Tables 1 and 2). Additional values outside of the computed and tabulated regions can be solved for from formulas given in the appendix of this reference.

With the above quantities defined and the shrouded propeller thrust given, an approximate solution of the flow field is possible. Any shroud with sufficient vortex strength distribution along its mean camber line to make up the computed deficit in the value of the stream function at the trailing edge of the shroud will, when added to the value of the stream function for the sink distribution, permit an approximate solution for a flow field. The unit stream surface of the above will pass through the trailing edge and the form outlined by the unit stream surface can be replaced by a solid body in the flow field. Hence, an approximate solution is assured. The problem is much more complex, however, in that a proper distribution of vortex strength must be made along a suitably positioned mean camber line in order to satisfy the condition of an assumed cylindrical wake and shroud contour expansion angle condition. In addition, an arbitrary shroud will not give inner and outer wake boundaries which even approximately coincide. As an illustration of this difficulty, which also exists for the case of the unshrouded rotor or propeller, Figures 4 and 5 are reproduced from reference 3.

Adaption of the Method of Singularities to the Design of Shrouds in Static Thrust.--As referred to earlier in this work, a proper selection of an assumed mean camber line for a proposed theoretical shroud is essential in satisfying certain boundary conditions. In this section attention is focused on the solution of this problem.

An angle between a vertical reference line passing through the trailing edge stagnation point and the tangent to the shroud at this point is defined as the shroud contour expansion angle. (See Figure 1) It has been found from the experience of others in shroud design that in the case of the shroud with a large free stream velocity, separation of flow along the inner contour of the shroud occurs if the angle of shroud contour expansion exceeds approximately 10°. A shroud without a free stream velocity, it has further been learned, may have a slightly increased angle of expansion without a flow separation along the inner contour of the shroud. This, then, establishes one of the criteria to be met.

The second consideration, introduced by the use of the tabulated values for the vortex cylinder, is a camber line position and a bound vortex strength distribution such that the wake variation from a cylindrical shape is negligible. All that is actually required is that the wake boundary remain cylindrical to a distance below the sink disk plane to a point beyond which effects of the variations from the cylindrical wake condition can be neglected.

With a given propeller thrust and wake boundary diameter, the strength of the wake bound vortex sheet, γ , can be determined from

$$T = Q\gamma; \quad Q = \rho\pi R_o^2 v = \frac{\rho\pi R_o^2 \gamma}{2} \; ; \quad \gamma = \sqrt{\frac{2T}{\rho\pi R_o^2}}$$

With the wake bound vortex sheet strength known, it was shown in Chapter II, section 2, that the deficit can be computed for any point along the wake boundary. It was also stated previously that the wake variation from a cylindrical shape must be minimized for a distance below the sink disk plane within which effects of said variation can not be neglected. Past experience, again, has shown that a reasonable distance below the sink plane is approximately $3R_o/2$. Therefore, if a shroud of proper dimension and position is designed which will make up the deficit along the wake boundary for a distance of approximately $3R_o/2$, the second stated criteria is satisfied. Concurrently, the reader is reminded that the shroud contour expansion angle limits are not to be violated. For example, if the bound vortex strength distribution is as shown in Figure 6, the wake condition is very nearly satisfied, but the bound vortex strength distribution along the assumed mean camber line is such as to cause an obviously excessive expansion angle, thus eliminating this particular distribution from the standpoint of a practical solution. It will be shown later that the outer stream surface can be adjusted considerably, whereas the inner contour is relatively immovable thereby ruling out the shroud of Figure 6 as a possible solution.

With several variables to be considered simultaneously, and working in three dimensions, establishing a workable procedure has been one chiefly of trial and error. The most feasible sequence encountered in this study is one where, first the deficits at the trailing edge, and at one-half assumed wake radius intervals, to three-halves assumed wake radius below the plane of the sink disk plane, are computed. Next an arbitrary mean camber line is assumed. The author, in this study, found

that it was necessary to assume a mean camber line with a length of approximately R_o to obtain a shrouded airfoil of reasonable thickness. An approximation to a continuous distribution of bound vortex strength along the mean camber line of the shroud can be made by selecting vortex rings of proper strength at one-quarter R_o intervals (or less for greater accuracy) along the mean camber line. The values of the stream function, including the increments from these spaced vortex rings, are then obtained by computing values of Ψ at points lying along planes midway between spaced rings in the flow field and subsequently fairing the total Ψ curve and joining points of equal value to obtain the desired stream surface (see Figure 7).

Initially, the mean camber line is assumed to be a straight line of length R_o beginning at the initially selected reference point, the trailing edge. Distribution of bound vortex strength approximated by finite strength rings to be discussed subsequently, is spaced at $R_o/4$ intervals (or less) along the mean camber line. Beginning with position 1 of Figure 8, the flow field is plotted to establish an outline of the unit stream surface, which forms the inner contour of the proposed shroud.[1] As only an approximation is necessary to determine the general form of the inner contour at this time, it is suggested that a minimum number of points be plotted to save time and effort. Concurrently with plotting the inner contour of the shroud, the stream surface is determined

---

[1]It will be later noted that the dimension assumed is not the true length of the mean camber line, merely the distance of the furthermost vortex ring along the mean camber line. The true dimension of the shroud will vary with the position of the mean camber line and the distribution of the bound vortex strength along same.

at selected points below the plane of the sink disk. This process is repeated for each of several positions[1] shown in Figure 8. The process is necessarily time-consuming; hence, as stated previously, it is suggested that only a minimum number of points be plotted initially to establish the inner contour and that the wake shape be checked at $R_o/2$ intervals up to $3R_o/2$ below the plane of the sink disk for several positions shown in Figure 8.

Before the above computations can be accomplished, however, a suitable distribution along the assumed mean camber line must be made. A discussion of bound vortex strength distribution can be found in reference 2, which is also applicable to the design of shrouds in the case of static thrust. Without a detailed treatment of the subject of bound vortex strength distribution, it should be apparent that each type of distribution will yield a differently shaped shroud and that an infinite number of possible distributions exist. From this study it was determined that a suitable distribution was one as shown in Figure 9. Distribution of bound vortex strength was computed directly by determining the strengths necessary at points Γ_1, Γ_2, Γ_3, and Γ_4 to make up equal portions of the total deficit at the trailing edge of the shroud. The deficit at the trailing edge is $\pi R_o^2 \gamma/2$, therefore, the amount of total deficit to be made up by Γ_1, Γ_2, Γ_3, and Γ_4 is $\frac{\pi R_o^2}{8}$

---

[1]It was found that the limits of positions shown in Figure 8 bound an acceptable solution for a length of the mean camber line of R_o. A position of the assumed mean camber line that is too vertical will cause the computed value of the stream function to violate the shroud contour expansion angle condition. Too large an inclination will alter the wake boundary, forming wake shapes differing considerably from a shape which is cylindrical.

The increment of fluid contributed by each ring varies with the distance from the trailing edge and the radius of the ring (reference 1). Therefore the strength of each ring will be

$$\frac{\pi R_o^2}{\Delta\psi_n 8}$$

where $\Delta\psi_n$ is the increment of nth ring per unit strength ring having unit radius.

When the inner contour has been sketched in, and the wake boundary checked for each of several positions shown in Figure 8, a selection of the position most nearly meeting the required conditions is made.

Further improvement in both wake boundary shape and shroud contour expansion angle can be obtained when the assumed, straight mean camber line of the shroud is replaced by a parabolic curve, or some other suitable curve.

With the above procedure accomplished, the value for the desired stream function is plotted, paying particular attention to the inner contour of the shroud and to the wake shape to obtain an accurate plot. For reasons to be brought out in the next section of this chapter, dealing with thickness distribution, the outer contour of the proposed shroud can be sketched in roughly at this point in the design.

To recapitulate the basic steps of the procedure of shroud design covered in this section, the following outline is presented:

1. From the initial conditions, compute γ and select a mean camber line dimension.
2. With distribution as shown in Figure 9, or some other suitable distribution, select the best straight line

camber line by iterating through several of the positions shown in Figure 8.

3. Fit a suitable curve to the end points of the straight line with the best inclination and repeat iteration for one position on each side of the originally selected camber line.

4. Plot the desired stream surface for the best suited mean camber line.

With the above performed, the unit stream surface with resemble the form shown in Figure 10.

Utilization of Known Inner Contour Surfaces as Corresponding Inner Surfaces of Theoretical Shroud.--When the steps outlined in the preceding sections of this chapter have been completed, the (x, r) field is plotted for regions in the vicinity of the unit values of the stream surface and the contour of the shroud is determined. In the general case, the resulting shape will resemble the form shown in Figure 10.

If the inner surface of this shroud could be "fitted," that is, expanded into a slightly altered shape, it would be possible to utilize either a standard NACA airfoil section, or use the formula given in reference 4 for the computation of airfoil sections, and determine a section of desired thickness. Utilization of known airfoil sections in this manner would be very desirable in that it would permit using shapes which are known to have smooth pressure distributions for the important inner contour of the theoretical shroud.

Measuring maximum thickness of the shroud in a direction perpendicular to the mean camber line one may, at this point, select a NACA wing section, or compute one, whose inner contour is slightly thicker than the shroud contour obtained in the previous section.

This selected thickness distribution for the inner shroud contour can be laid out along the mean camber line of the theoretical shroud.

Professor Walter Castles, Jr. and Robin B. Gray have developed a method of shroud thickness distribution which is sufficiently accurate to allow the desired inner contour fitting (see reference 2). Pairs of closely spaced vortex rings of opposite sign are placed well inside the thickness of the shroud. In general, it has been found to be good practice to place the pairs perpendicular to, and straddling, the mean camber line. The number of pairs used, strengths, and locations along the mean camber line are completely arbitrary as long as they are well inside the thickness of the shroud. The effects, however, of the more closely spaced pairs are local in nature whereas a widely spaced pair will have an influence over a large region of the flow field. Further, a distribution of weaker but more numerous vortex pairs will tend to resemble a continuous distribution along the mean camber line and will yield improved results. It is advisable to begin the fitting process from an extension of the mean camber line position (see Figure 11) and work down toward the trailing edge of the shroud. Quite obviously, the effects of all pairs set out must be superimposed on the original flow pattern, the contour of the desired stream surface adjusts itself accordingly, and the fitting process is in this manner accomplished.

During the fitting process, as well as observing carefully the inner contour of the designed shroud, attention must be paid to the wake boundary to assure little or no change from a cylindrical flow shape. Variation of the location, strengths, and spacings of the vortex pairs utilized in the fitting process will permit one to do this. As the

trailing edge of the shroud is approached with pairs of vortex strengths during the fitting procedure, and having properly fitted the upper portion of the inner contour, it is advantageous to position the plus vortex ring and the minus ring in any position straddling the mean camber line, which will produce the desired balanced total strength of the flow field in the vicinity of the trailing edge and in the wake. For example, it may be found helpful to reverse the positions of the plus and minus rings in order to adjust the values of ψ at the trailing edge to the desired value of ψ total.

When an acceptable adjustment of the inner contour of the theoretical shroud has been made, the stream surface outlining the shroud contour is carefully plotted for the outer surface. The shape will resemble the form shown in Figure 2.

If a horizontal plane is passed through the originally selected trailing edge,[1] and neglecting all portions of the shroud below this plane, a shroud shown in Figure 2 will remain. The form outlined, then, is one which can be replaced by a solid body in the flow field.

Since the stream function of the shroud is known and the velocity components of the flow can be determined from tables or computed for any point along the surface of the shroud, it follows that Bernoulli's Theorem will permit computation of pressures along the shroud surface[2]

---

[1]It is not necessary to pass a horizontal plane through the reference point, the trailing edge, as shown in Figure 2. The designed shroud may be "cut off" from its determined unuseable portion at any point desired.

[2]Pressure distribution formulas given are approximate since the number of propeller blades is finite and the rotational component of velocity, V_t, due to torque, has been omitted.

where

$p_o - p = \frac{1}{2} \rho (V_x^2 + V_r^2)$ for points ahead of the propeller and

$p_w = \frac{1}{2} \rho \gamma^2 + p_o$ is substituted for p_o for points behind the propeller, and within the wake.

CHAPTER III

RESULTS

Figure 2 shows a form of a shroud obtained as a final result of procedures outlined in Chapter II. It is apparent from methods discussed that, as a consequence of the fitting process, identical initial conditions may produce various shaped shrouds. This is possible since the shape of the outer contour is dependent upon the amount of expanding that is necessary for coincidence of the theoretical and the desired inner contours. Therefore, the selected airfoil section, to a great extent, determines the overall form of the shroud and the resulting solution is not unique. Another way of varying the designed shroud shape is to plot a stream surface slightly greater than unity. These contours will have a reduced thickness at the plane of the disk.

The stream surface below the plane of the sink disk converges, gradually, to an extension of the assumed cylindrically shaped wake (see Figure 2). Since it would be impractical to construct a shroud of such dimensions and shape, an arbitrarily established cut off plane is passed through the designed shroud and a useable portion of the entire shroud outline, lying above said plane, is thereby fixed. In Figure 2, the arbitrarily selected plane also passes through the trailing edge point of the shroud. The form remaining, above the plane, in Figure 2, is one which in practice can be replaced by a solid body. The inner contour of this solid body is that of either a standard NACA or computed airfoil section. The significance and importance of this result

lies in the fact that the most important portion, the inner contour of a propeller shroud, can be related to airfoil sections for which the coordinates are readily available.

To determine pressures along the surface of the designed shroud entails the application of Bernoulli's Theorem, using the equations, and the restrictions on said equations, given at the end of Chapter II.

CHAPTER IV

CONCLUSIONS

The results of this study show that an approximate theoretical solution can be obtained for the design of a static thrust propeller-shroud combination utilizing the method of singularities. The following assumptions were made: (a) steady flow, (b) axial symmetry, and (c) incompressible flow. It is further concluded from the results of this study that procedures outlined in this report furnish a practical method for designing propeller shrouds. The procedures outlined, though necessarily lengthy, are quite readily understandable and relatively simple to apply.

CHAPTER V

RECOMMENDATIONS

In order to determine the extent of the possible increase in shrouded propeller efficiency that can be obtained by using the shroud design method given in this report, it would be desirable to run wind tunnel tests on a propeller-shroud combination designed by this method and compare the results with previous tests.

From practical considerations, a strictly static thrust shroud has limited applications. The other extreme, a high speed device, can be viewed in the same light. A possible continuation, or an extension of the work undertaken here, is the investigation of a propeller-shroud combination design which would fulfill both static thrust and high speed requirements or would yield a compromise solution.

Table 1. Final Computed Values, Theoretical Shroud

Point	Ψ	Point	Ψ	Point	Ψ
E-2	941	G-5	835	C-3	1094
D-2	988	C-4	1048	A- 2 1/2	881
C-2	930	F-5	932	A- 2 5/100	830
A-2	816	E-5	1028	A'- 2 1/10	846
E-6	908	D-5	1023	A'- 2 1/2	850
B-4	976	D-4	1151		
G-3	834	B-3	945		
A'-2	817	F-4 1/2	997		
E-1	449	E-4 1/2	1117		
D-1	448	A-3	911		
C-1	502	A'-3	862		
H-3	579	C'-3	840		
G-2	432	C'-2	832		
H-4	621	B'-3	853		
G-4	928	B'-2	845		

1. See Figure 12(h) for reference system used.

2. Values shown include Ψ value due to bound vortex strength distribution and Ψ_s combined, computed as shown in example computation, Appendix.

3. Points, above, are considered minimum number to determine form desired (other points, not shown, were plotted in sample computation of Appendix).

Table 2. Final Computed Values of Ψ for Vortex Ring Pairs

Point	(300) (A)	(300) (B)	(300) (C)	(100) (D)	(100) (E)	(100) (F)	(75) (A')
E-2	-12	-30	+03	+24	-02	0	
D-2	-15	+54	+03	-15	-09	-10	
C-2	+18	+54	-09	-22	-14	+04	-04
A-2	-06	0	0	-08	-04	-06	+12
E-6	0	-	-27	-	-	-	
B-4	-51	-30	-15	-28	-21	-21	
G-3	-09	-24	+06	+32	-51	+57	
A'-2	-12	0	0	-06	-05	-03	+04
E-1	-06	+03	-03	+04	+06	+04	
D-1	-12	+06	0	-05	-01	+05	
C-1	+09	+06	-03	-04	-04	-03	
H-3	+15	-09	-09	+02	+02	+06	
A'-2 1/2	-03	-09	0	-06	-03	-06	+07
G-2	-06	+45	+12	+03	+15	+14	
H-4	-15	+45	-15	-07	-12	-03	
G-4	-15	-03	-30	-11	-04	+06	
G-5	-12	-24	-42	-19	-40	-32	
C-4	-69	-78	-48	-37	-26	-15	
F-5	-09	-27	-30	-30	-34	-63	
E-5	-33	-33	-12	-48	-56	-66	
D-5	-15	-42	-12	-48	-51	-45	
D-4	-33	-27	0	-52	-55	-55	
B-3	-63	-42	-12	-16	-20	-13	+11
F-4 1/2	0	0	-	-30	-30	-74	
E-4 1/2	-39	-	-06	-57	-28	-77	
A-3	-45	-15	-03	-18	-14	-16	
A'-3	-15	-18	-06	-09	-07	-07	
C'-3	-06	-12	-12	-05	-05	-02	
C'-2	-06	-03	-03	-04	-05	-01	
B'-3	-24	-09	-03	-08	-06	-03	
B'-2	-08	-06	+03	-04	-02	-01	
C-3	-60	-72	-36	-30	-20	-03	-05
A-2 1/2	-30	-12	-15	-08	-08	-01	+07
A-2 5/100	-06	0	0	-09	-03	-02	+04
A'-2 1/10	-12	0	0	-06	-02	-02	-02

1. Reference system as shown in Figure 12(g).

2. Figures in parenthesis are strengths of vortex ring pairs of circled locations shown in columns above. Last column, (A') , is the vertically positioned pair as shown in Figure 12(g).

3. All columns are the combined effects of the pair indicated in parenthesis.

4. Only points influenced by vertical pair are shown in (A') column.

Table 3. Combined Totals of Tables 1 and 2

Point	ψ	Point	ψ	Point	ψ
E-2	924	H-4	614	C'-3	798
D-2	996	G-4	871	C'-2	810
C-2	957	G-5	666	B'-3	800
A-2	816	C-4	775	B'-2	823
B-4	810	F-5	769	C-3	868
G-3	889	E-5	780	A-2 1/2	807
A'-2	805	D-5	787	A-2 5/100	822
E-1	457	D-4	884	A'-2 1/10	824
D-1	481	B-3	790	A'-2 5/10	819
C-1	479	E-4 1/2	874		
H-3	583	A-3	800		
G-2	515	A'-3	800		

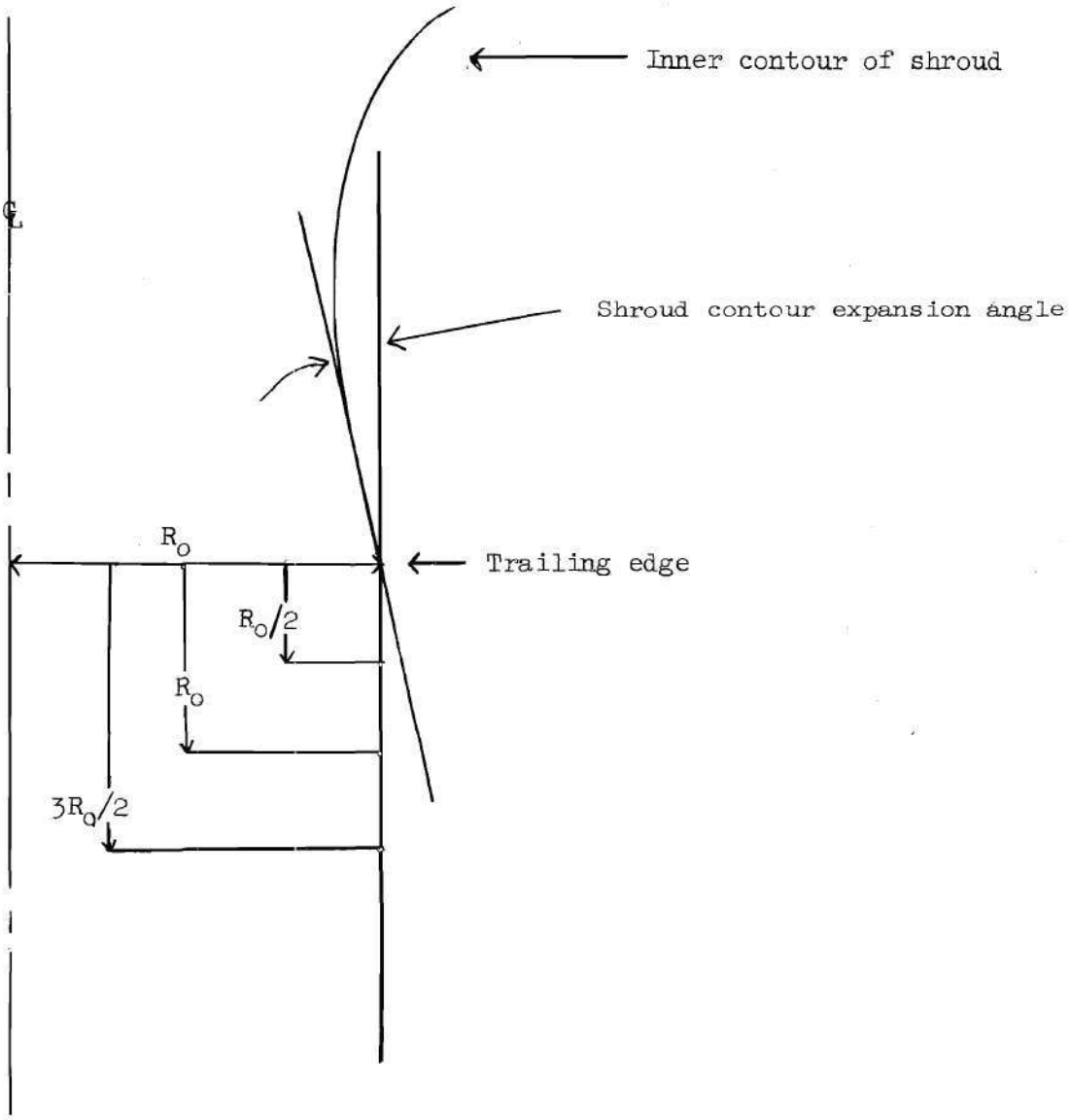

Figure 1. Shroud Contour Expansion Angle.

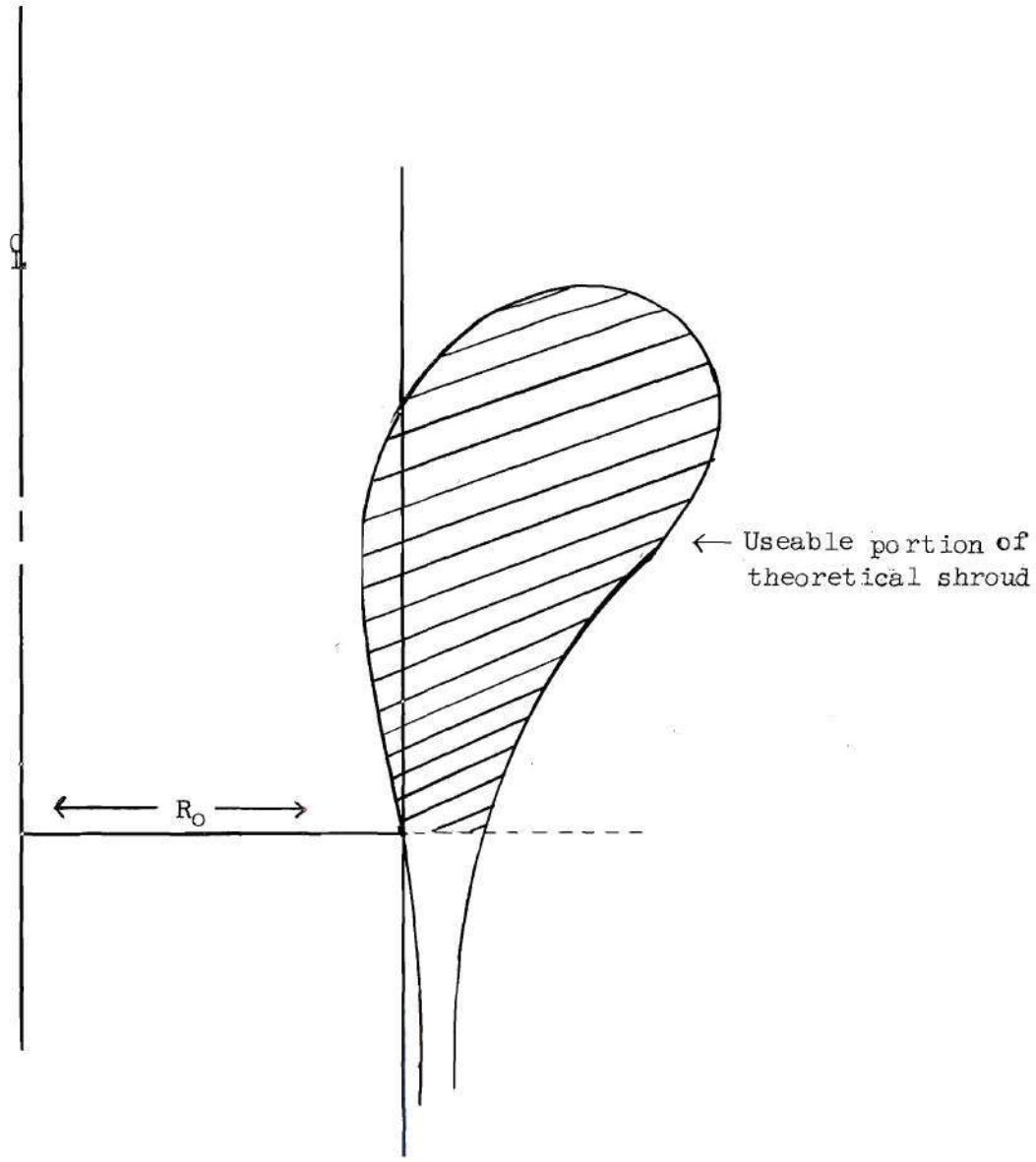

Note: Inner contour of the above shroud has been fitted to the desired inner contour of a known wing section.

Figure 2. Theoretical Solution Shroud Form.

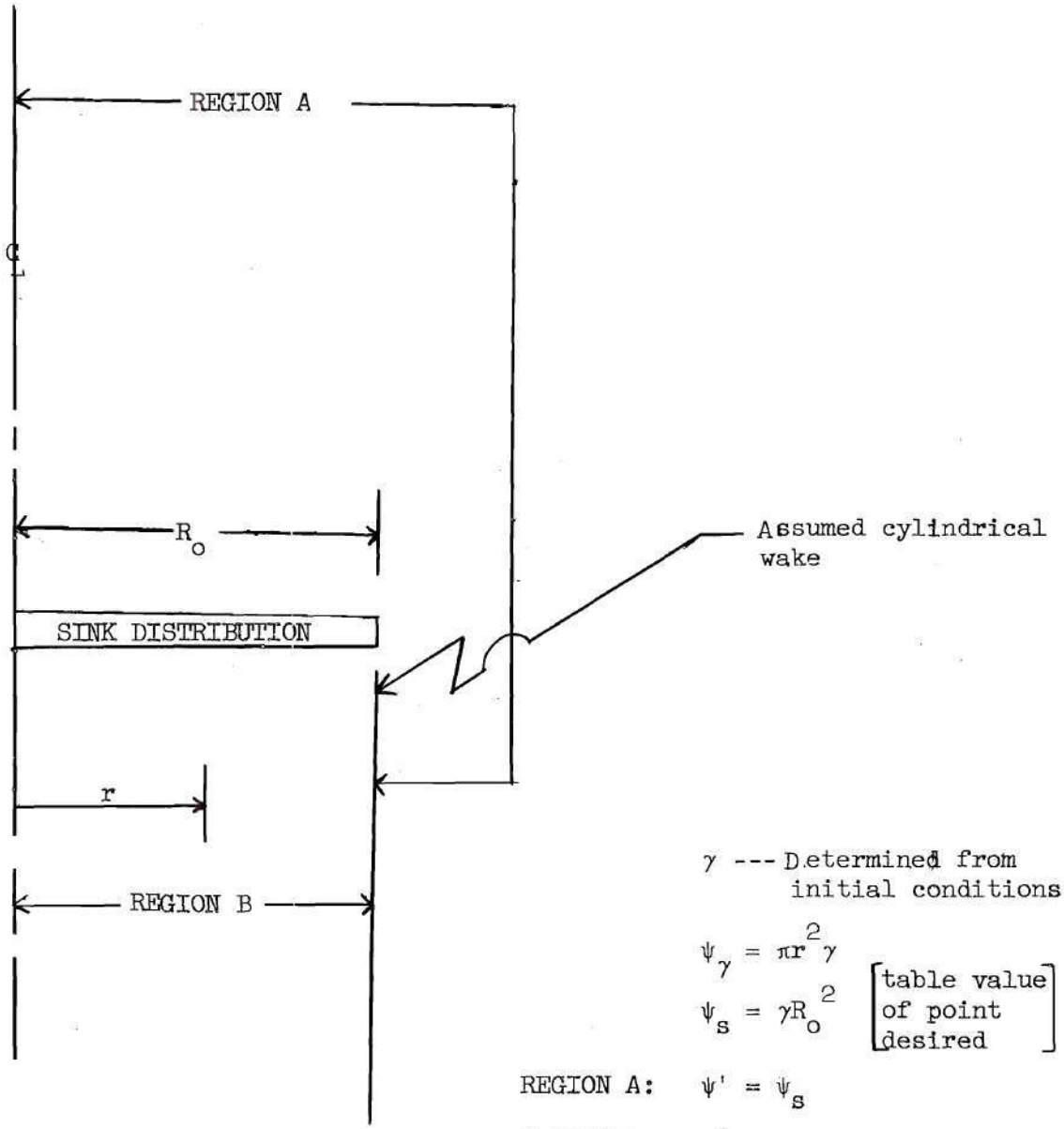

Figure 3. Regions of the Flow Field.

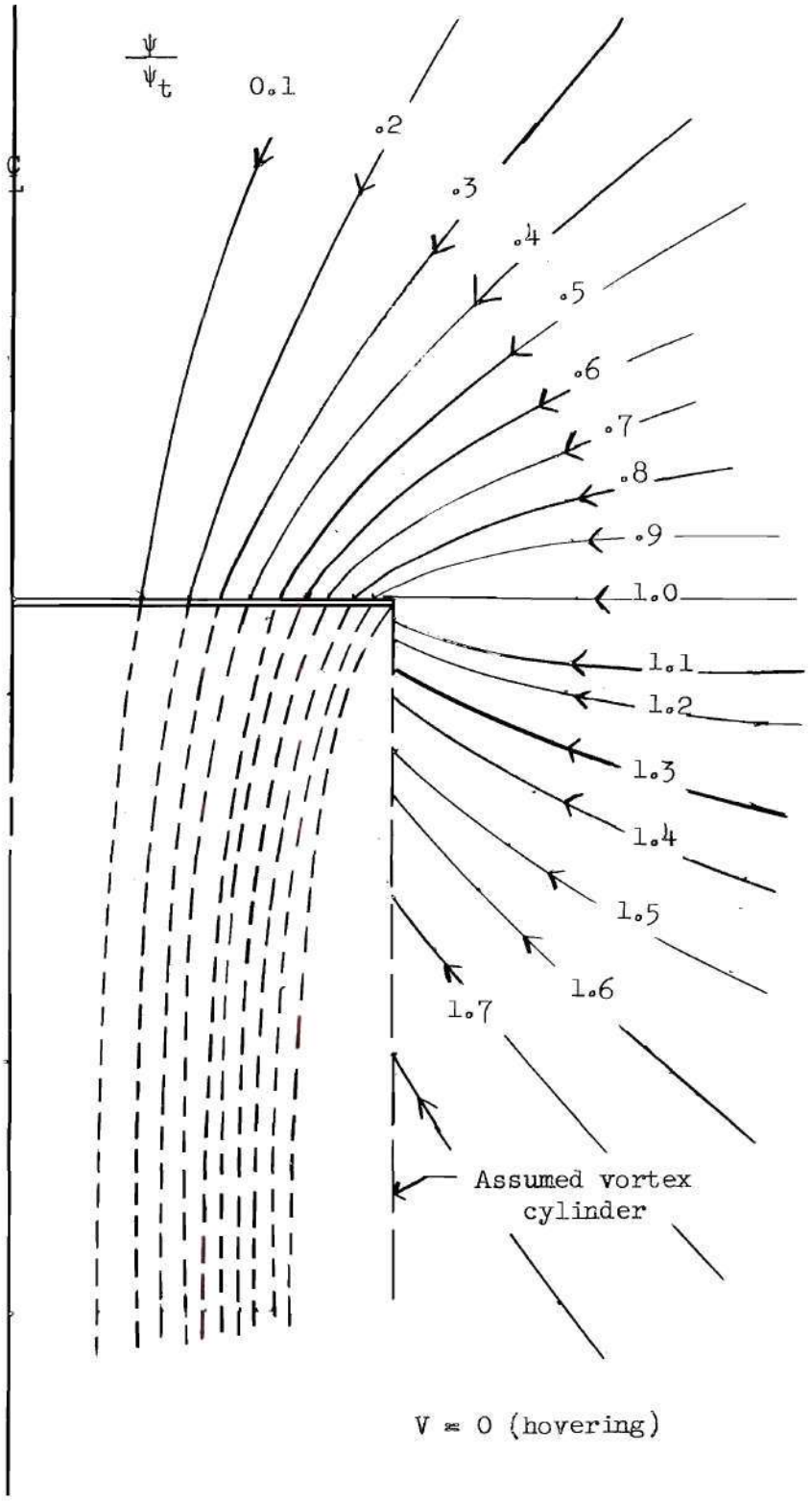

Figure 4. Streamlines for Wake Consisting of Uniform Vortex Cylinder.

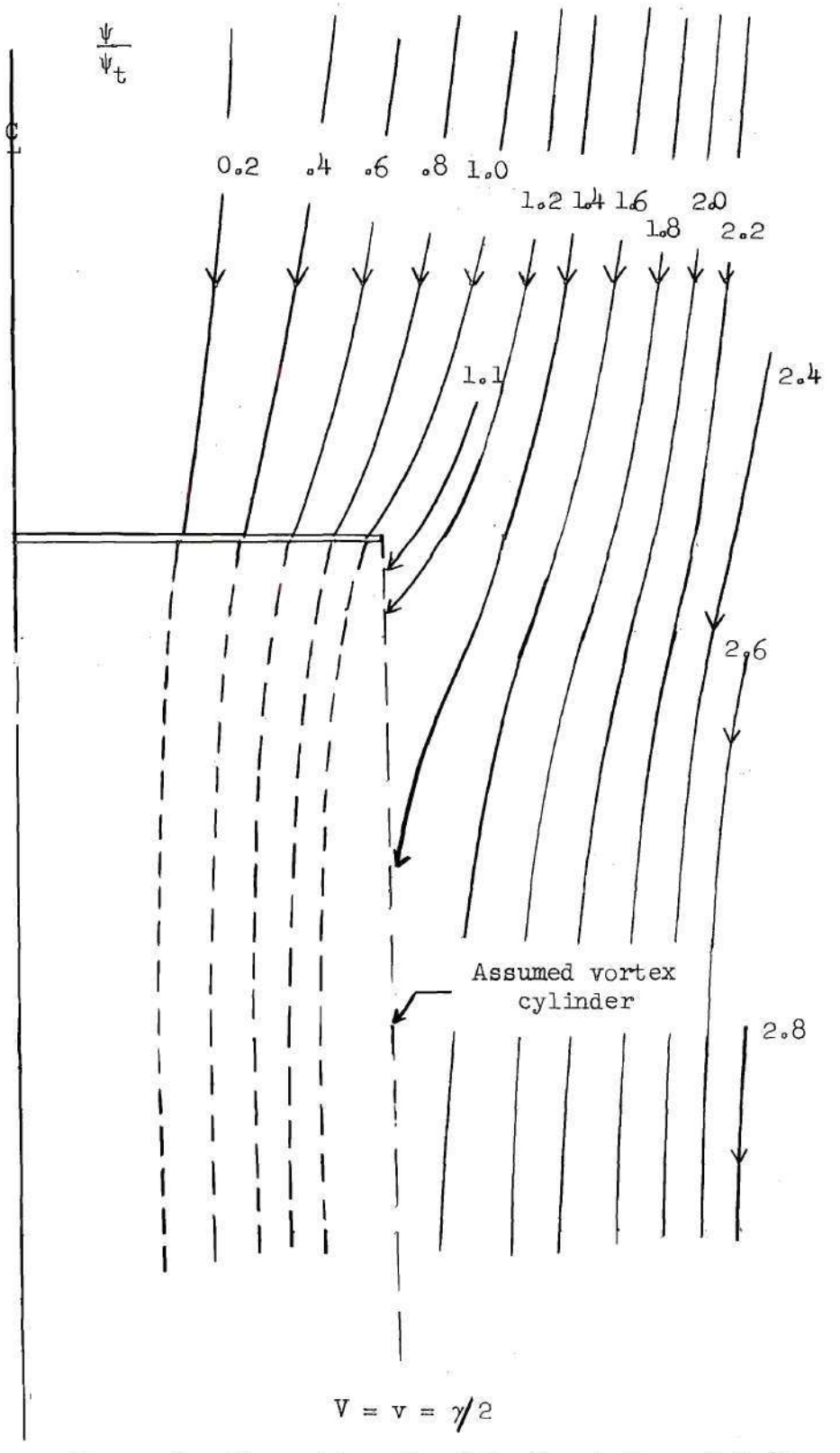

Figure 5. Streamlines for Wake Consisting of Uniform Vortex Cylinder.

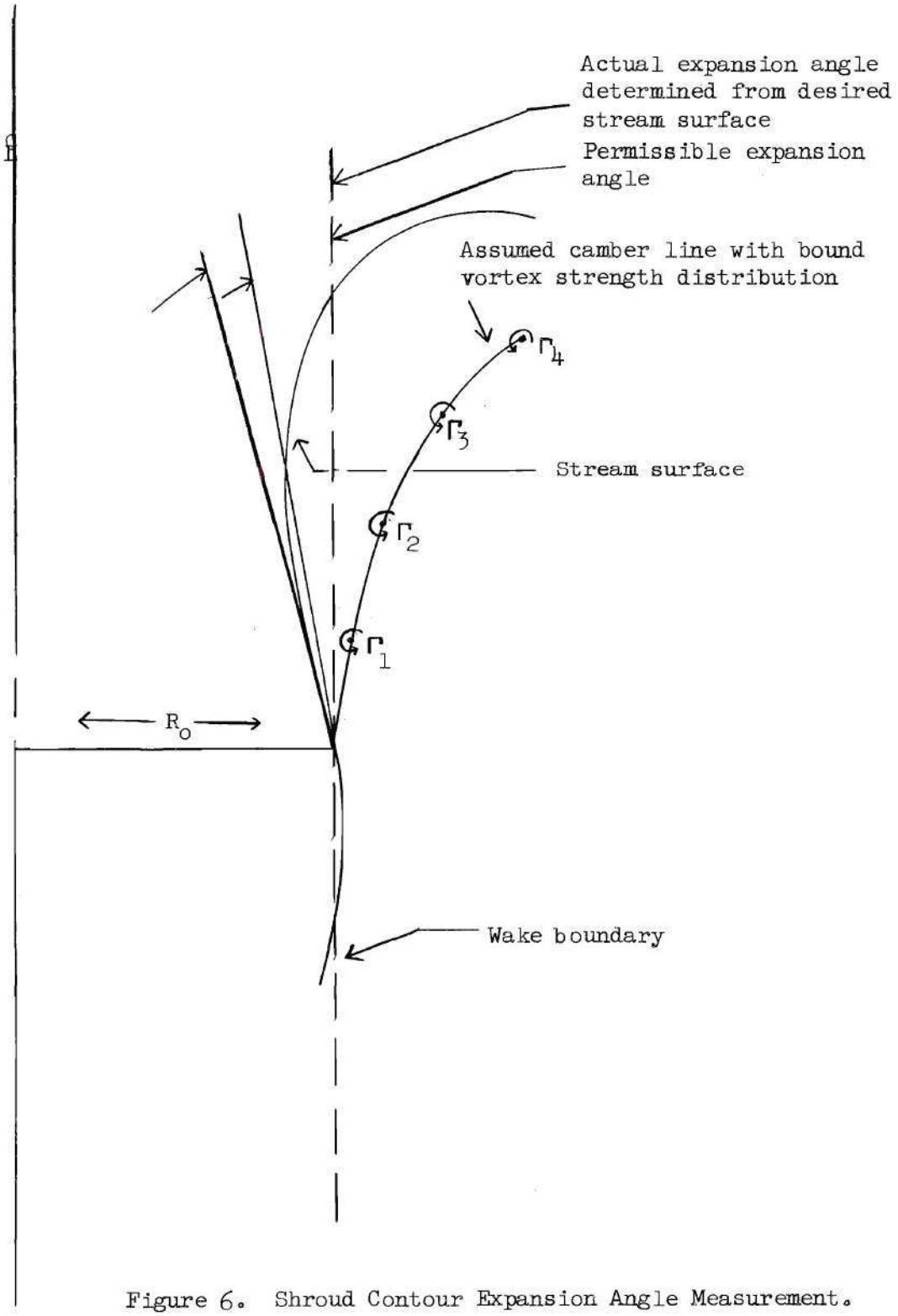

Figure 6. Shroud Contour Expansion Angle Measurement.

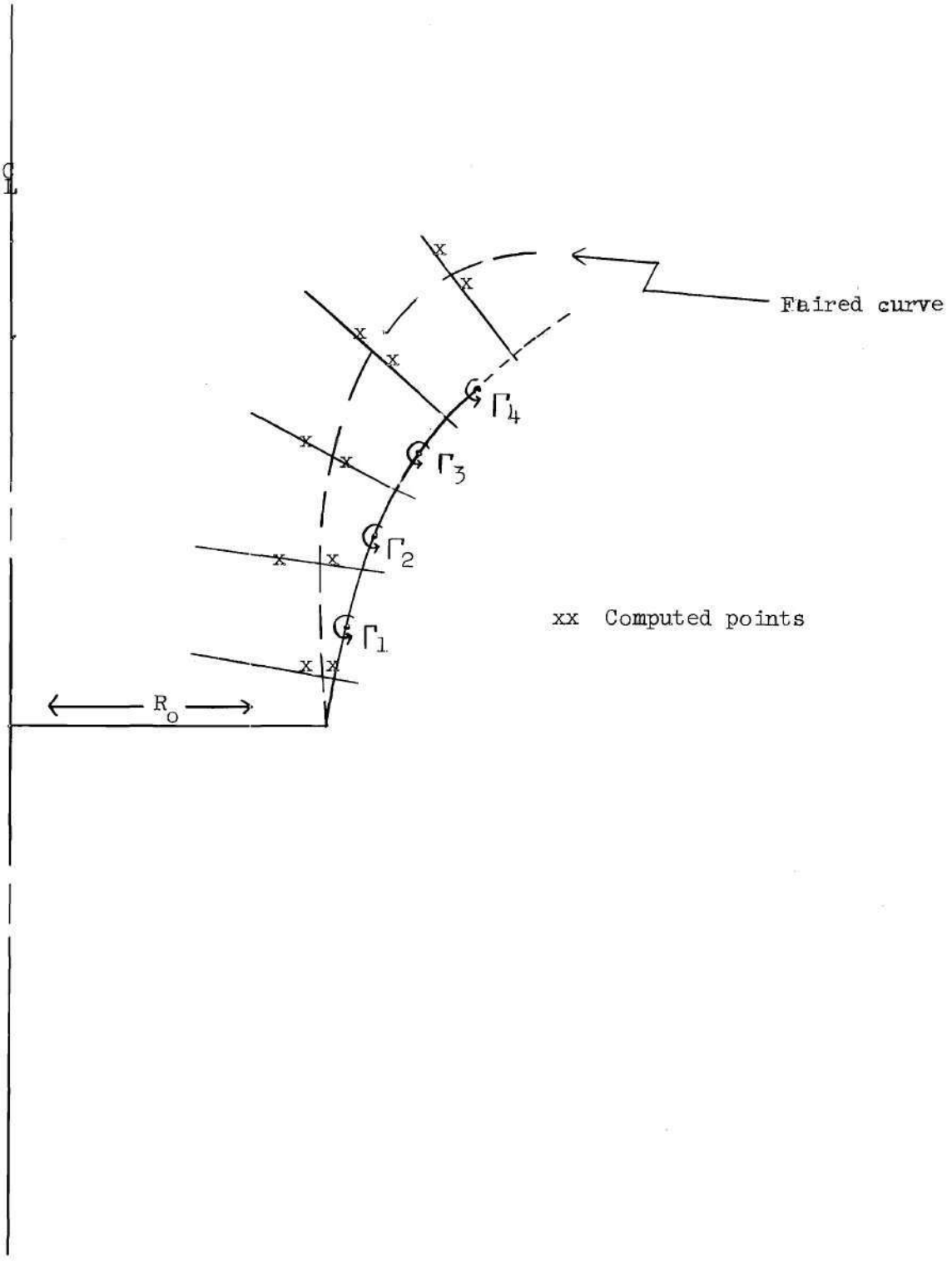

Figure 7. Planes of Computed Points.

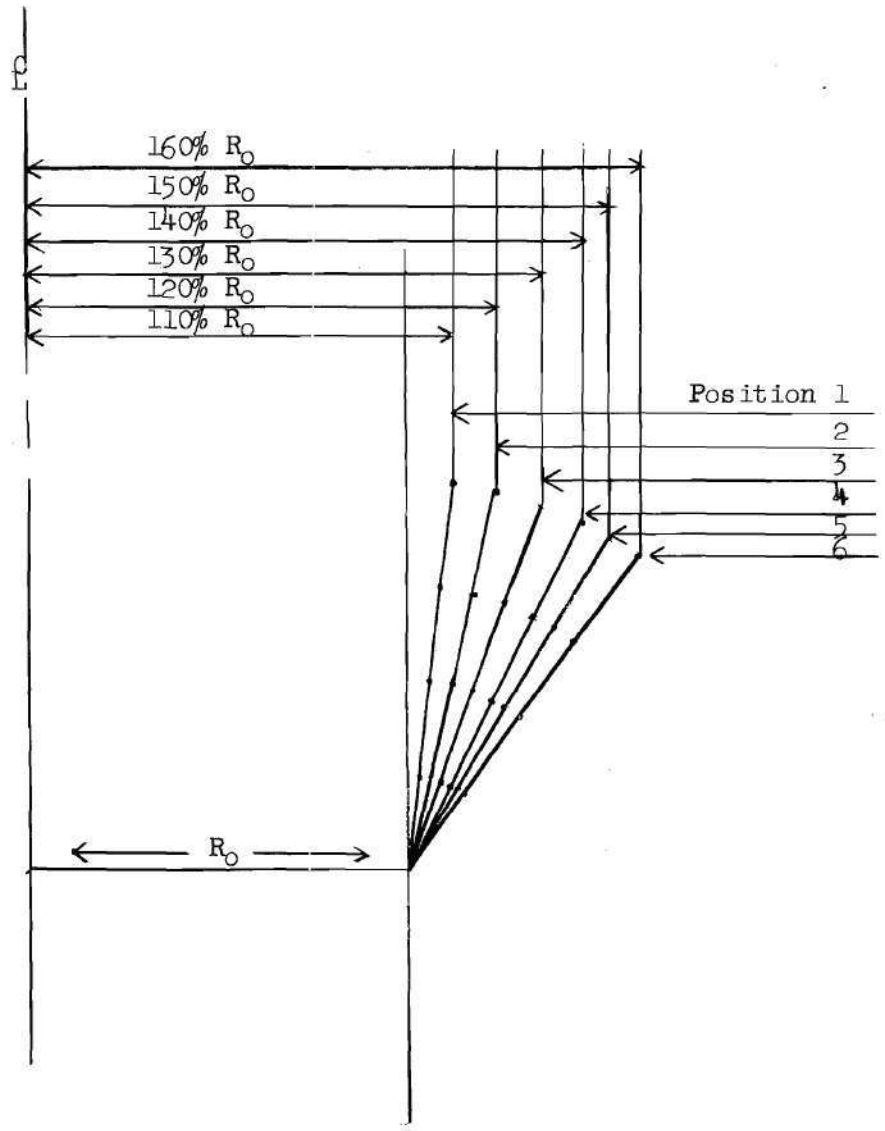

Figure 8. Iteration Positions of Mean Camber Line.

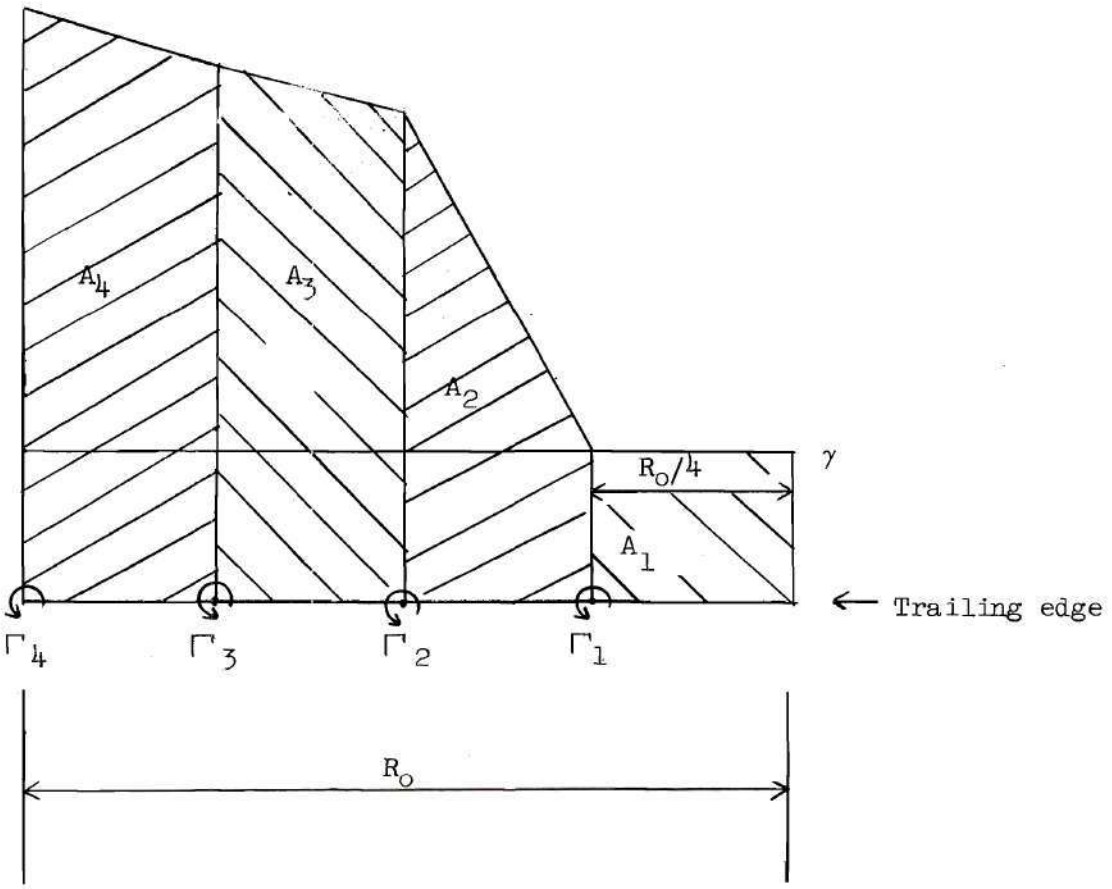

Figure 9. Shroud Bound Vortex Strength Distribution.

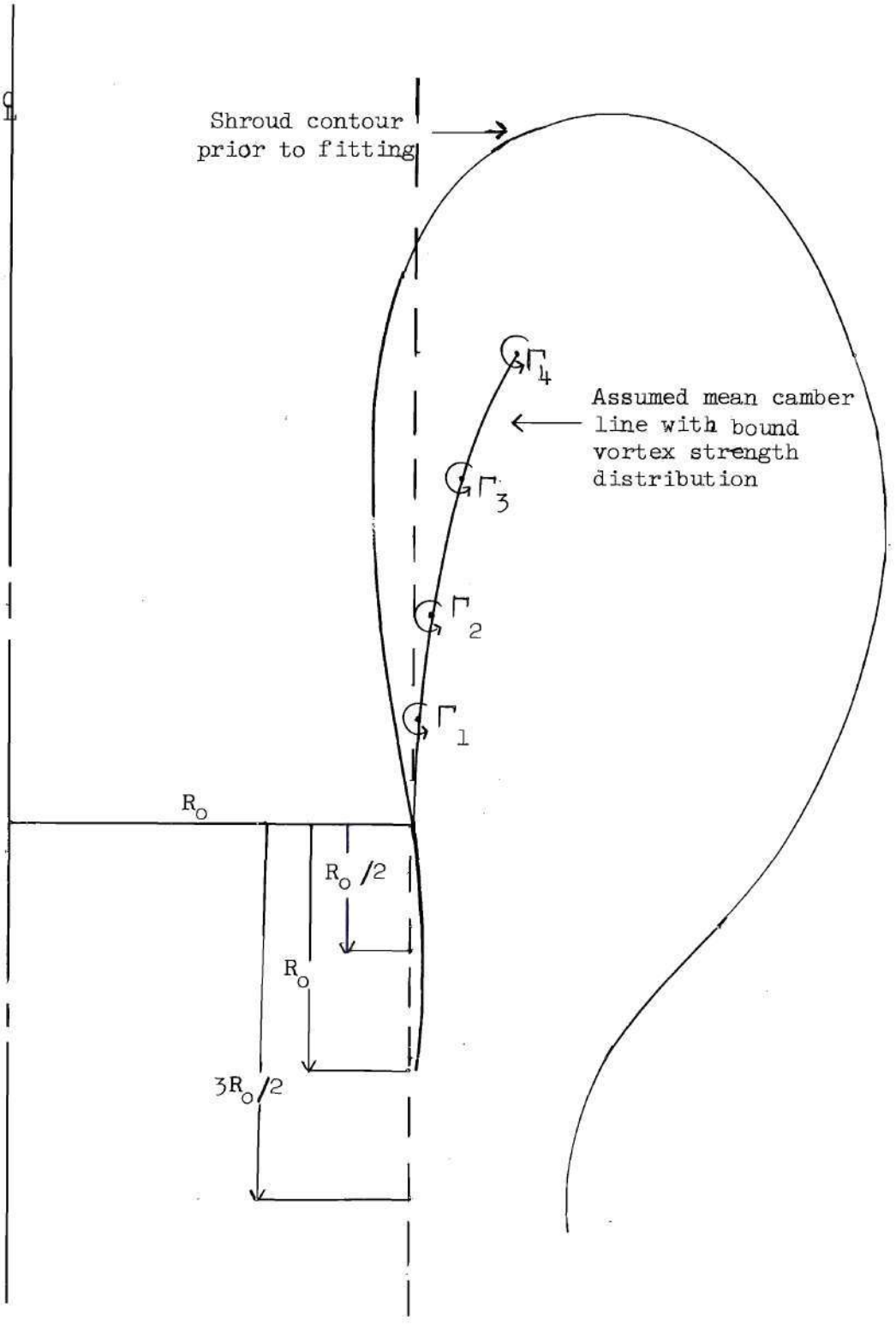

Figure 10. Shroud Form Including Shroud Bound Vortex Strength Distribution.

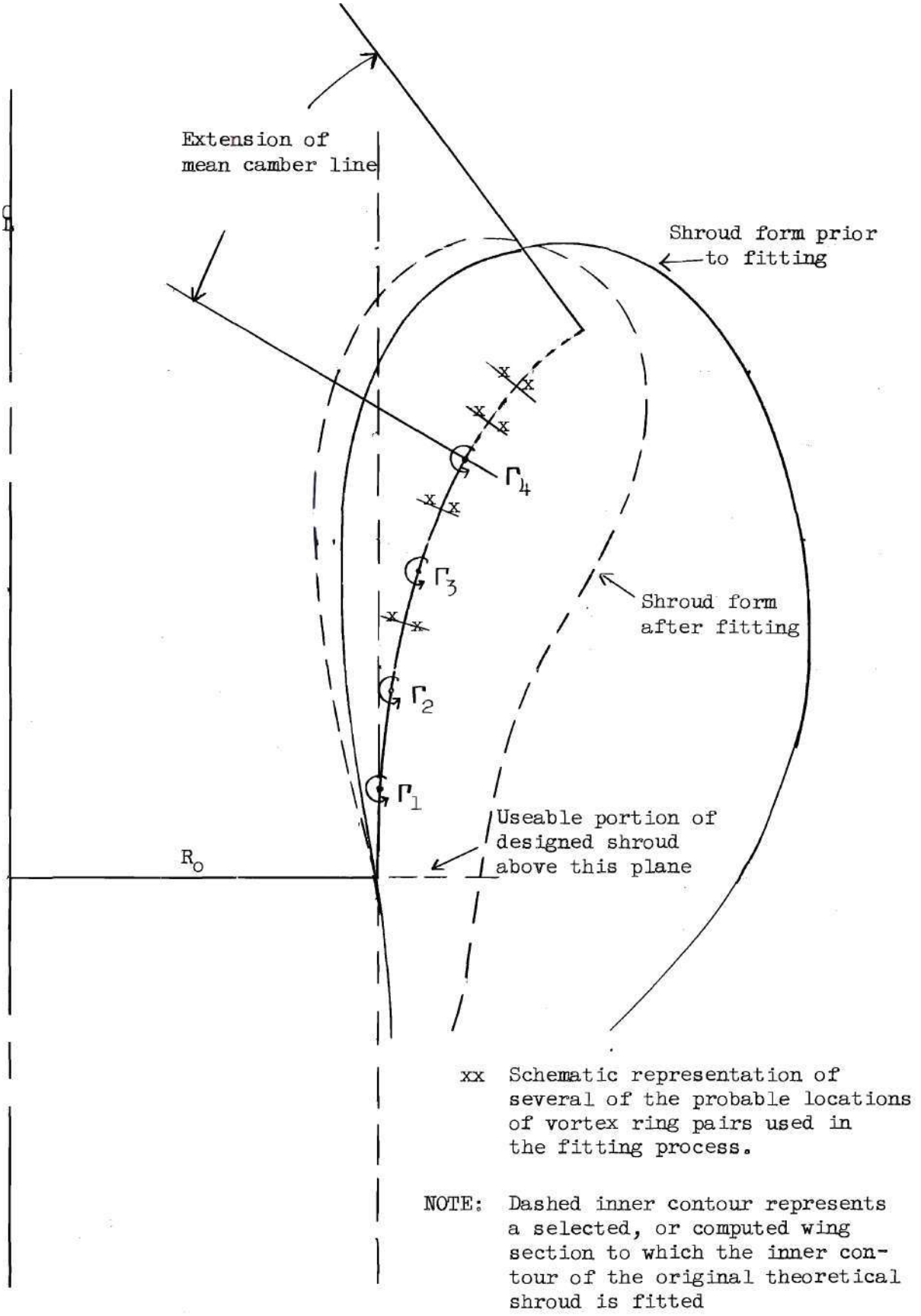

Figure 11. Example Locations of Vortex Ring Pairs.

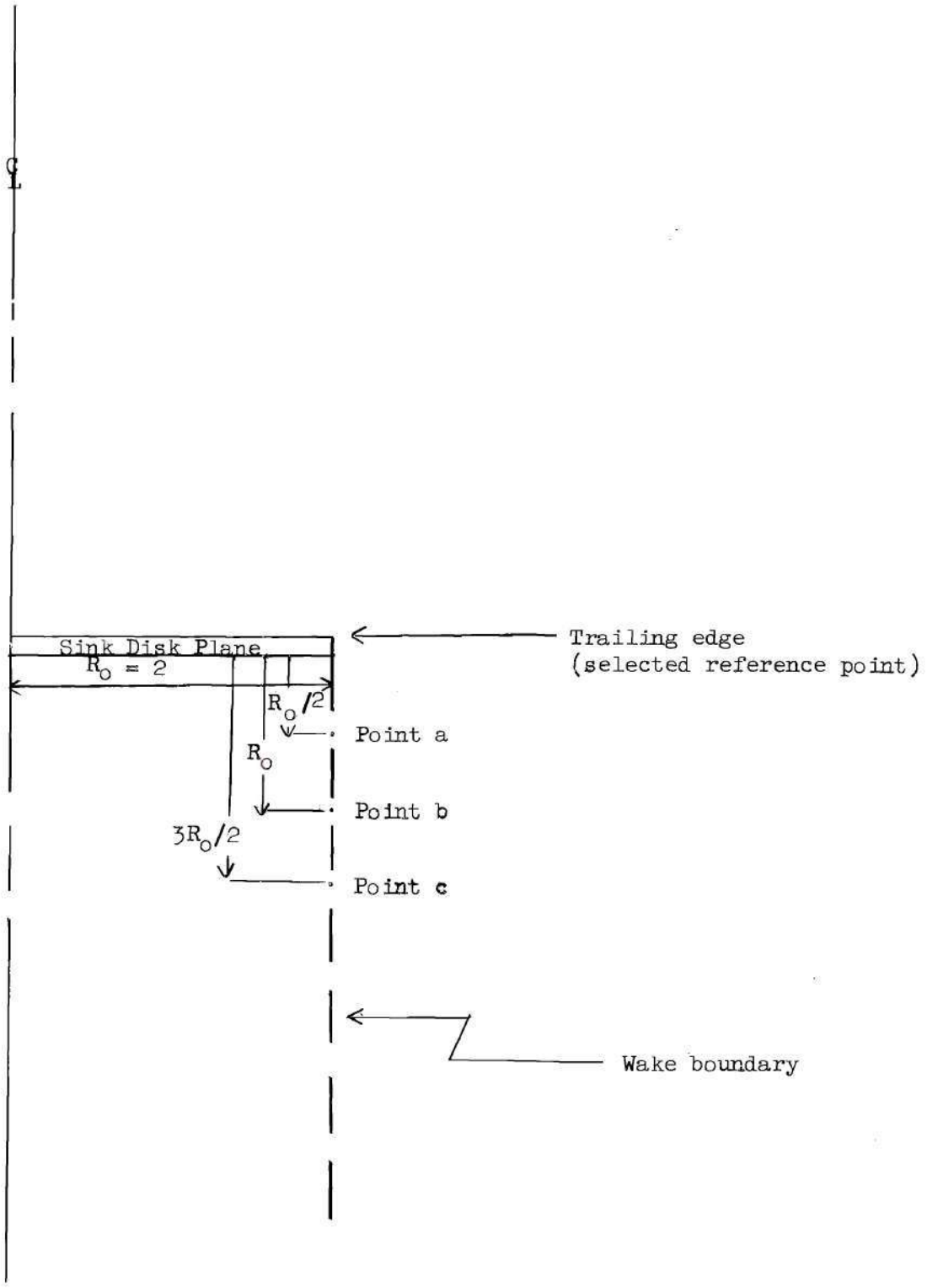

Figure 12(a). Reference Points, Sample Computation.

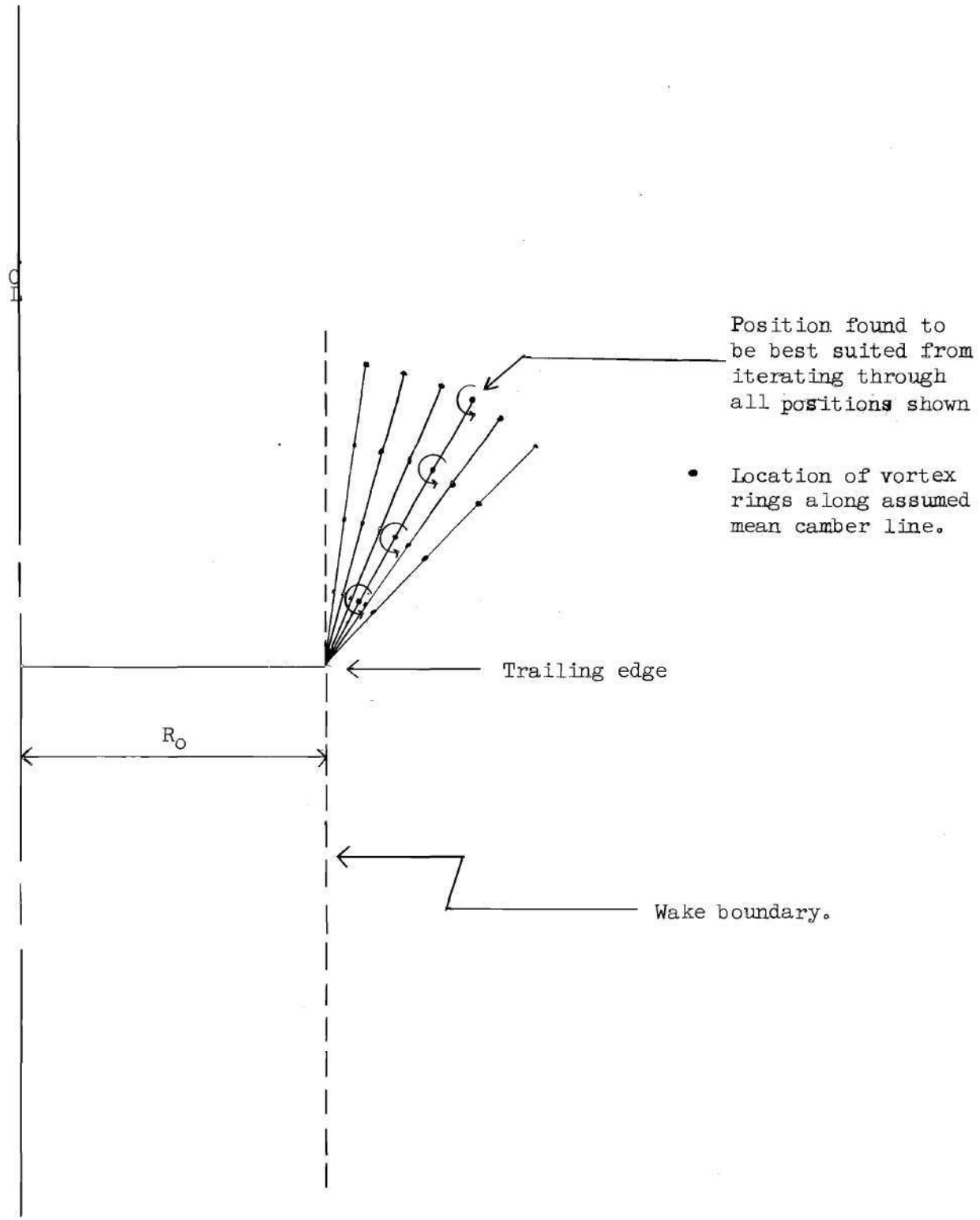

Figure 12(b). Iteration Positions, Sample Computation.

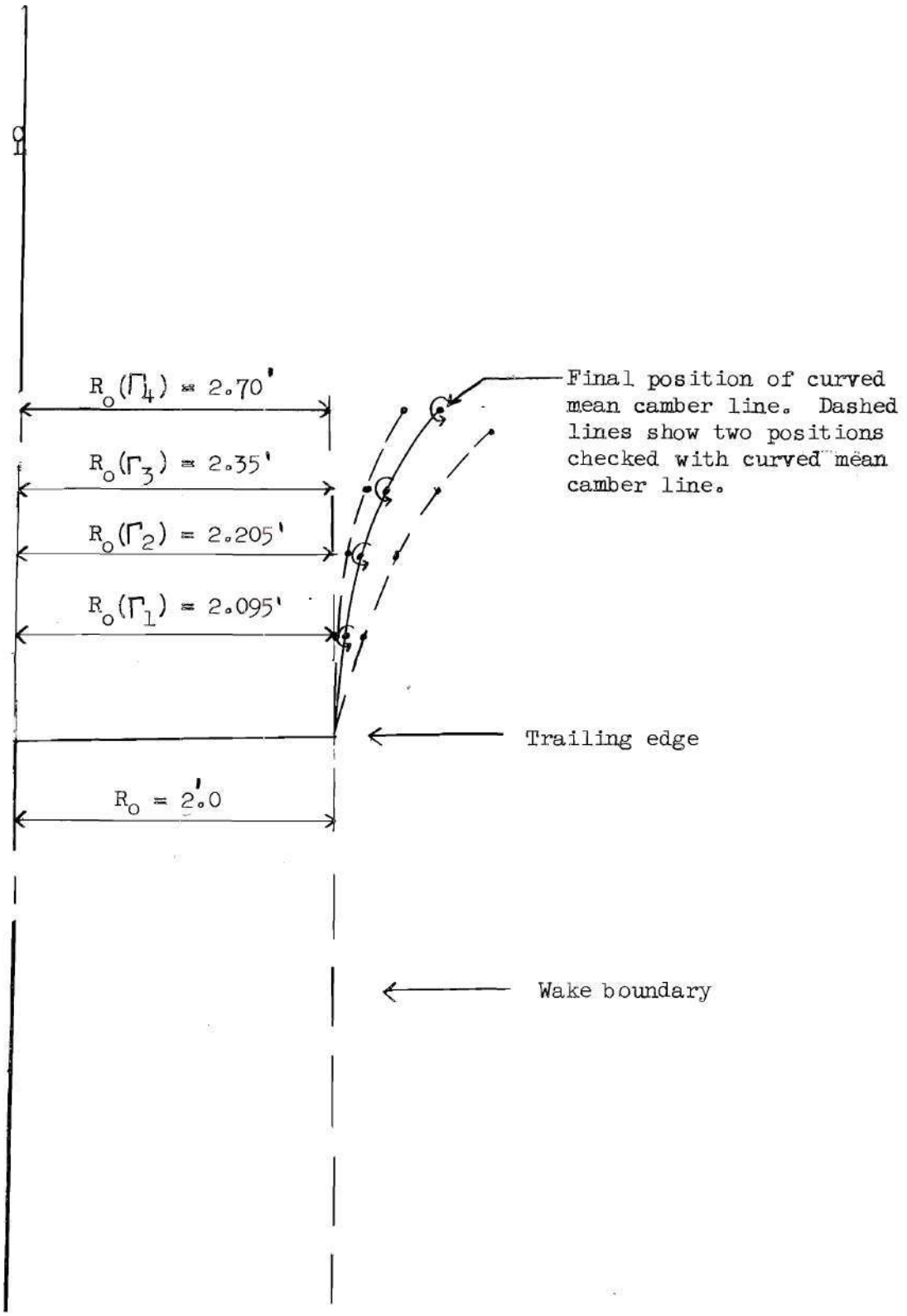

Figure 12(c). Final Iteration Position, Sample Computation.

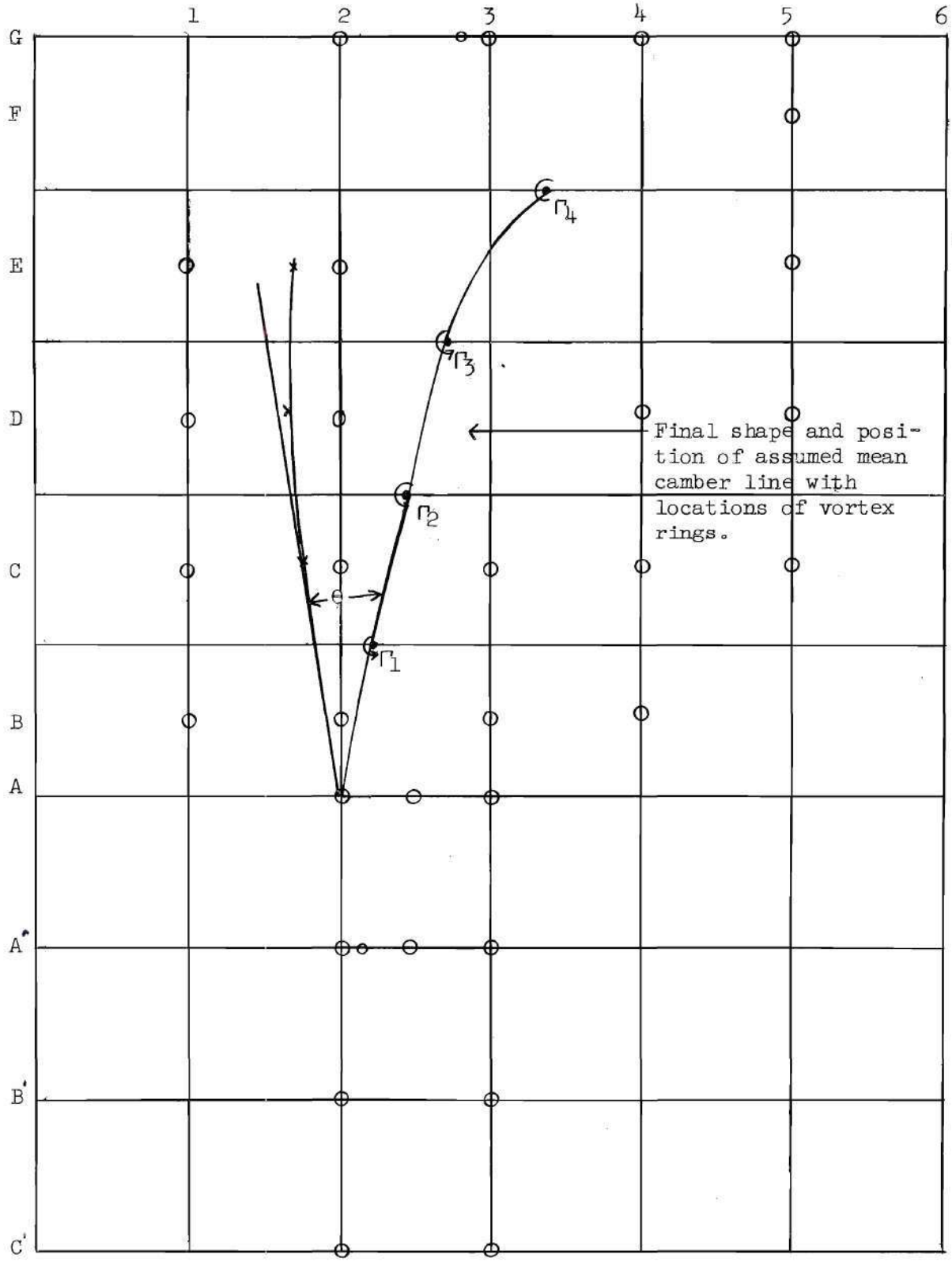

O - computed points. Sufficient length of inner contour is plotted to determine the shroud contour expansion angle: θ: $\tan^{-1} = .167$ $\theta = 9°30$

Figure 12(d). Computed Points, Sample Computation.

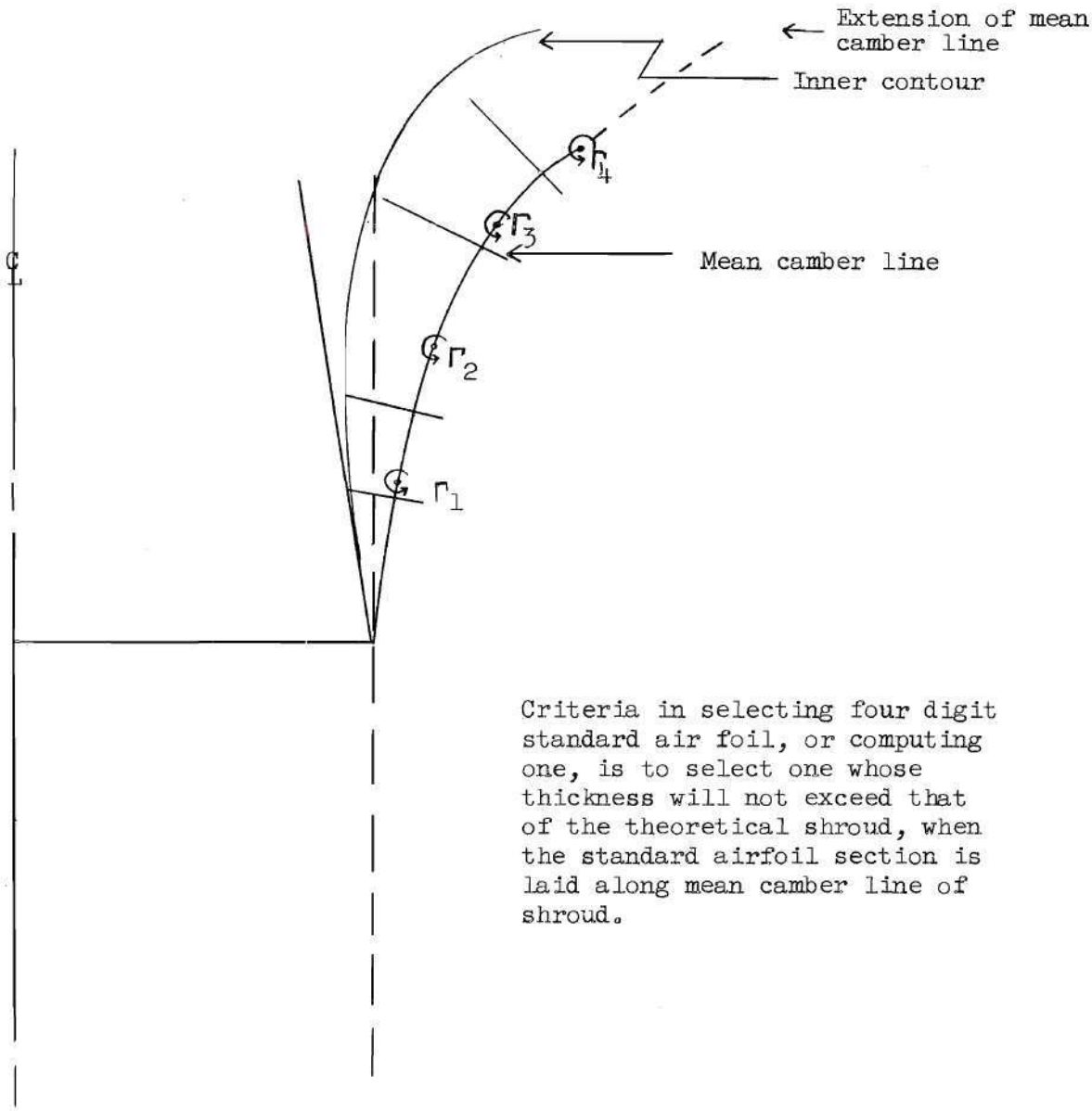

Figure 12(e). Schematic Representation of Maximum Thickness Measurement.

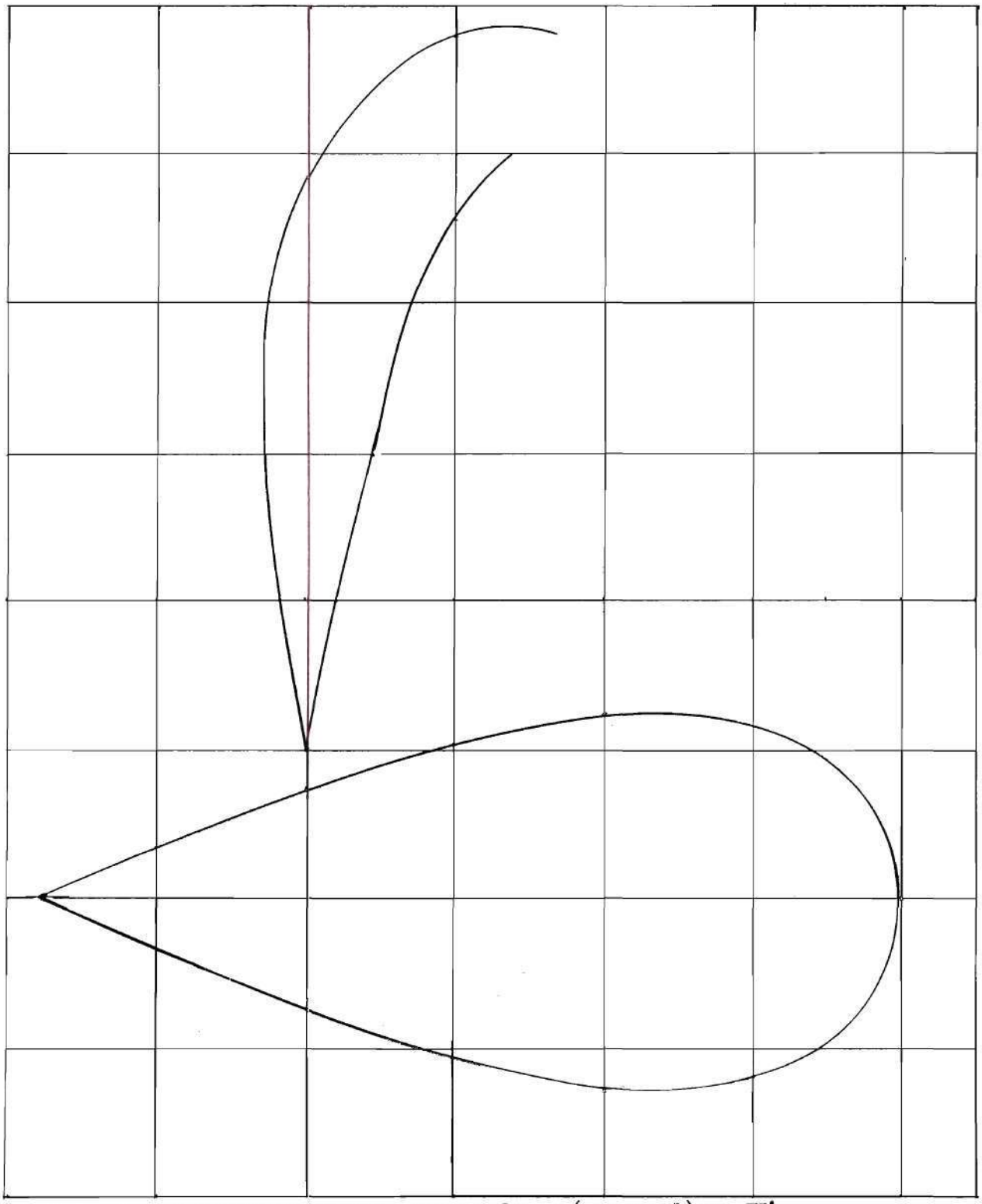

Lower figure - Compute airfoil section from y(measured) = .75'
Upper figure - Translated, computed section along finally determined mean camber line (inner contour)

Figure 12(f). Computed Wing Section, Sample Computation.

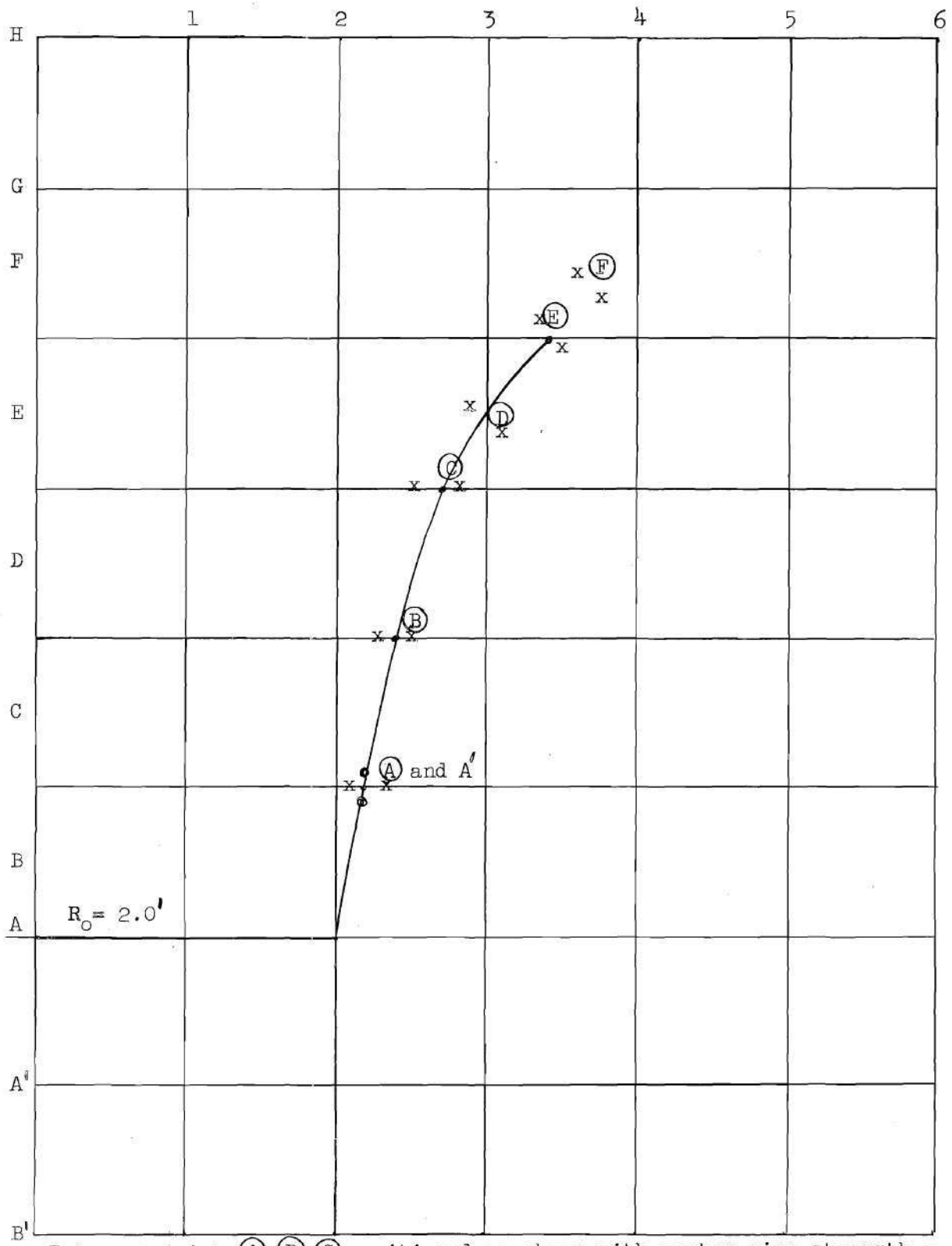

Pairs at points (A), (B), (C) positioned as shown with vortex ring strength = 300 each. Pairs at points (D), (E), (F), positioned as shown with vortex ring strength = 100 each. Final pair positioned at (A) (denoted as circles in Figure above); strength = 75 positions shown are to scale of: 1 square = 1.00" (+) rings all on left, (-) rings on right; vertical pair: (-) on top, (+) on bottom

Figure 12(g). Locations of Vortex Pairs, Sample Computation.

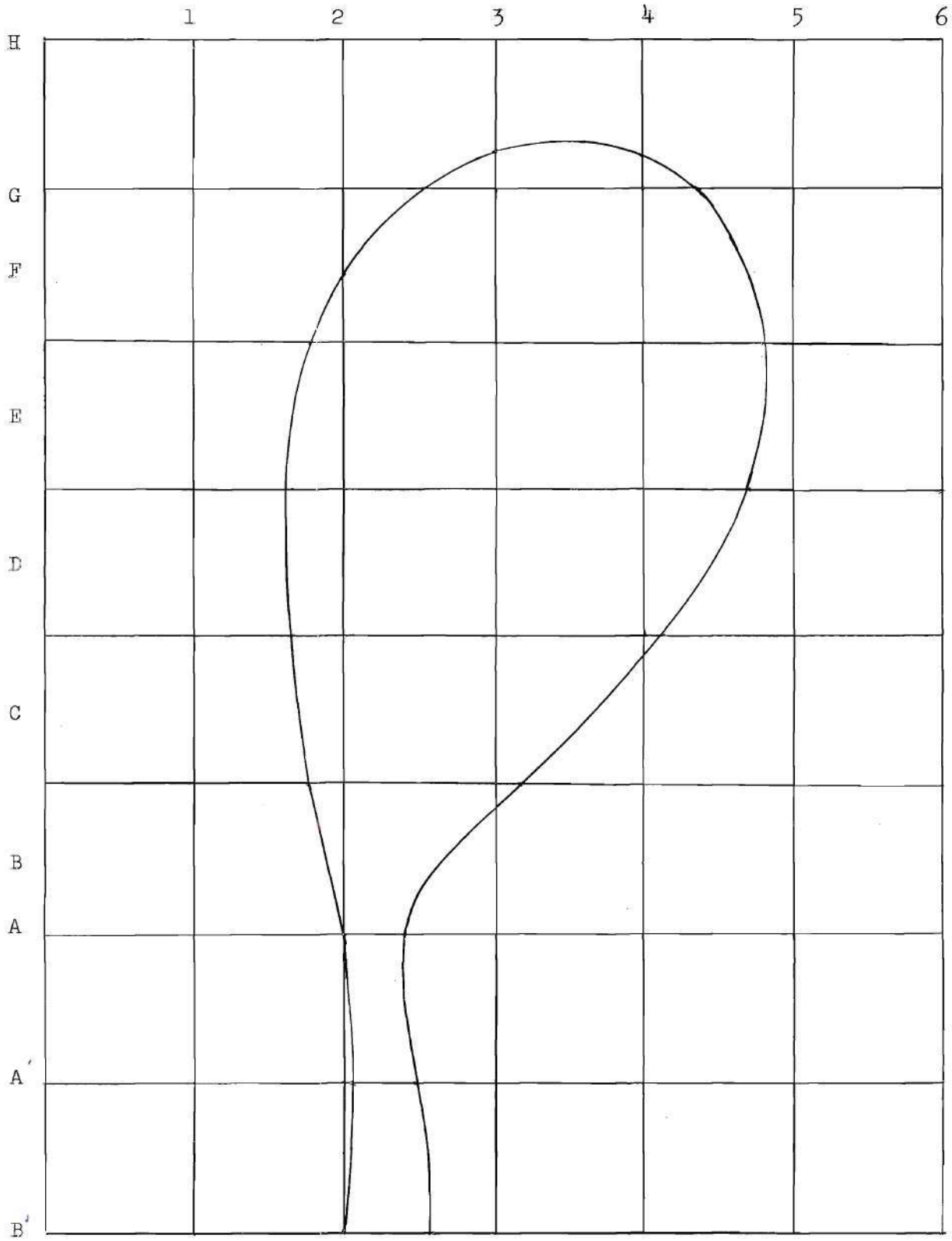

Figure 12(h). Theoretical Solution Shroud, Sample Computation.

APPENDIX

APPENDIX

Sample Calculation.--The detailed computations of this example are considered too voluminous to be included in their entirety; therefore only a minimum of example computations are shown here, with more consideration given to explanation of procedures used.

The general assumptions outlined in Chapter I hold in the following sample calculation and further it is assumed that it is desired to design a propeller-shroud combination for a propeller thrust of 5 lbs/ft^2 and a wake radius of 2 ft.[1]

$$Q = \rho \pi R_o^2 v = \frac{\rho \pi R_o^2 \gamma}{2} \qquad \text{where } \rho = .002378 \text{ slugs}/ft^3$$

$$T = Q\gamma; \quad \gamma = \sqrt{\frac{2T}{\rho \pi R_o^2}} = \sqrt{\frac{2(5)\pi R_o^2}{.002378\ \pi R_o^2}} \; ; \; \gamma = 65/\text{ft sec}$$

$$\Psi \text{ (of the ultimate wake)} = \pi R_o^2 \gamma = \pi(2)^2(65); \; \psi = 816 \; ft^3/\text{sec}$$

As a beginning point in the design of a theoretical shroud for the above conditions, select a reference point, the trailing edge of the shroud, as shown in Figure 12(a).

Since $\psi = \pi R_o^2 v = \frac{\pi R_o^2 \gamma}{2}$ at the trailing edge, the amount of fluid needed to adjust the deficit to zero at this point is $\frac{\pi R_o^2 \gamma}{2} = 408 \; ft^3/\text{sec}$.

---

[1] It should be noted that the shape and contour of streamlines are independent of disk loading due to the fact that no free stream velocity exists.

Select three points below the horizontal plane containing the selected reference point, the trailing edge, (denoted as points a, b, and c in Figure 12(a)) and compute the deficit at each point. This deficit quantity will be computed for one point, point 2 only, as an example.

Since the uniform vortex cylinder is replaced by a uniform distribution of sinks over a disk (Figure 12(a)), Table 17 of reference 1 may be used to obtain $\Delta\psi_s = .96$ for $x/R_o = \frac{5}{2}$ and $r/R_o = \frac{2}{2}$. Note that point a is below the sink disk plane, hence, from symmetry considerations, as indicated in Figure 3, this value must be subtracted from π . Then

$$\psi_s = (3.14 - .96)\gamma R_o^2 = 541 \text{ ft}^3/\text{sec}$$

ψ(total) was determined as 816 ft^3/sec.

Therefore, deficit at point a is $816 - 541 = 275 \text{ ft}^3/\text{sec}$

In a similar manner, the deficit of any point along the wake boundary may be computed. It is to be noted that the amount of deficit diminishes below the sink disk plane, approaching zero in the ultimate wake, and that the deficit existing along the wake boundary must be adjusted to zero at each point by the designed shroud, if the shape of the wake is to remain cylindrical.

Next, the distribution of bound vortex strength along an assumed mean camber line must be made. For this example, assume a straight line length of 2 feet from the trailing edge to the position of the furthermost vortex ring position, Γ_4 (see Figure 12(b)). As discussed

in Chapter II, a suitable distribution was one as shown in Figure 9, determined as follows

$$\text{Deficit at the trailing edge} = \frac{\pi R_o^2 \gamma}{2}$$

Four vortex rings, spaced at $R_o/4$ intervals (or less for greater accuracy) along the mean camber line, are used here. Therefore, the deficit to be made up by each of the rings is

$$\frac{\pi R_o^2 \gamma}{8} = 102 \text{ ft}^3/\text{sec}$$

The strength of Γ_3 is computed, here, as an example, using mean camber line position as shown in Figure 12(c). Table 3 of reference 1 gives a value of $\Delta\psi$ contribution to the trailing edge of

$$\Delta\psi = .575/\text{unit radius} \quad \text{or} \quad \Delta\psi = .575(2.35) = 1.353$$

Then,

$$\Gamma_3 = 102/1.353 = 75.2$$

In a similar manner Γ_1, Γ_2, and Γ_4 can be computed.

Then $\Gamma_1 = 32.5 \quad \Gamma_2 = 52.5 \quad \Gamma_3 = 75.2 \quad \Gamma_4 = 96.7$

With this distribution, each of the positions shown in Figure 12(b) were, in turn, checked to determine which most nearly fulfilled wake and expansion angle conditions. The indicated position of Figure 12(b), was found most suitable. The end points of this line, then, were fitted to a parabolic curve, $y = ax^2$, and again checked for one position on each side of the position indicated in Figure 12(b). The resulting mean camber line was one as shown in Figure 12(c). All points shown in Figure 12(d) were computed as follows (using point D-4 as an example).

	x/R_o	r/R_o	$\Delta\psi R_o$	$\Delta\psi R_o\Gamma$	ψ_s	$\psi_s + \psi_r$	$\div\ \psi_t$
Γ_1	.359	1.435	1.13(2.093)	76.6	$x/R_o = \frac{1.25}{2}$		
Γ_2	.113	1.360	1.45(2.205)	16.80	$r/R_o = 3/2$		
Γ_3	.106	1.270	1.63(2.35)	288.0	$\Delta\psi_s = .88$		
Γ_4	.278	1.110	1.49(2.70)	389.0	$(.88)(\gamma R_o^2) =$		
	Totals			921.6	229	1151	1.41

An inner contour shape as shown in Figure 12(d) resulted for the ψ total stream surface.

Fitting Procedure.--A maximum thickness, measured perpendicular to the mean camber line, is now determined for the inner contour of Figure 12(e) which will permit the shroud contour expansion angle a slight (arbitrary amount) increase in the fitting process.

In this example, a NACA 6_4-021 airfoil section could have been used. However, this airfoil would not have permitted much room for expanding the inner contour of the theoretical shroud into the standard airfoil. Therefore, it was decided to compute an NACA four digit wing section from the formula given in reference 4.

y(measured) = .75 ft and c(approximated) = 2.8 ft.

From the above $t = \frac{2(.75)}{2.8} = .535$

$$\pm y_t = \frac{t}{.2}\left[.2969\sqrt{x} - .126x - .3516x^2 + .2843x^3 - .1015x^4\right]$$

$r_t = 1.019t^2$ from reference 4.

giving an airfoil of desired thickness which, now, is laid along the mean camber line determined earlier and to which the inner contour of the theoretical shroud is now fitted (figure 12(f)).

Vortex pairs of strengths and positions as shown in Figure 12(g) were positioned along the mean camber line. Beginning from the top and working down toward the trailing edge along the mean camber line, a trial and error procedure was used to fit the inner contour of the theoretical shroud to the inner contour of the computed shroud. The effects of all pairs of vortex rings were computed for all points shown in Figure 12(d) and superimposed on the original flow field. For example, returning to point D-4, used earlier as an example point: At D-4, the original ψ value from shroud bound vortex distribution= 1151

Effect of vortex pair placed at A, Figure 12(g) is	-33
Effect of vortex pair placed at B, Figure 12(g) is	-27
Effect of vortex pair placed at C, Figure 12(g) is	0
Effect of vortex pair placed at D, Figure 12(g) is	-52
Effect of vortex pair placed at E, Figure 12(g) is	-55
Effect of vortex pair placed at F, Figure 12(g) is	-55
Effect of pair placed at A in a vertical position	-45
Total	884

Dividing by $\psi_t(816)$: $\frac{884}{816} = 1.08$.

Repeating the above for each point shown in Figure 12(d), and plotting the results, a shroud form such as is shown in Figure 12(h) is determined.

The final values of computed points, for the above sample calculation, are included in this thesis as Tables 1, 2, and 3.

BIBLIOGRAPHY

1. Kucheman, D. and Weber, J., Aerodynamics of Propulsion, 1st Ed., New York: McGraw Hill Book Co., Inc. 1953.

2. Castles, W. and Gray, R., An Investigation of an Approach to The Problem of Determining the Optimum Design of Shrouded Propellers, Project No. 9R 38-01-017-24, Contract No. Da-44-177-TC-402, Job Order No. 2, U. S. Army Transportation Research Command, Engineering Experiment Station, Georgia Institute of Technology, Atlanta, Georgia, May, 1960.

3. Castles, Walter Jr., Approximate Solution for Streamlines About a Lifting Rotor Having Uniform Loading and Operating in Hovering or Low Speed Vertical-Ascent Flight Conditions, NACA TN 3921, Washington, 1957.

4. Abbott, I. H. and Von Doenhoff, A. E., Theory of Wing Sections, corrected version of first edition, New York: Dover Publications, Inc., 1959.